Coordination Chemistry Reviews 254 (2010) 1826–1842

Contents lists available at ScienceDirect

Coordination Chemistry Reviews

journal homepage: www.elsevier.com/locate/ccr

Review

Active transition metal oxo and hydroxo moieties in nature's redox, enzymes and their synthetic models: Structure and reactivity relationships

Guochuan Yin*

School of Chemistry and Chemical Engineering, Huazhong University of Science and Technology, 1037 Luoyu Road, Wuhan, Hubei 430074, China

Contents

ARTICLE INFO

Article history:
Received 17 July 2009
Accepted 26 January 2010
Available online 2 February 2010

Keywords:
Metal oxo
Metal hydroxo
Reactivity difference
P450 enzyme
Xanthine oxidase
Lipoxygenase

ABSTRACT

The high oxidation state transition metal oxo moieties in redox enzymes and their models are generally recognized to serve as the key active intermediates in a series of hydrogen abstraction, oxygen transfer, and electron transfer processes. New evidence suggests that certain transition metal hydroxo moieties also play key roles in oxidative processes in biological and chemical systems. Clarifying the structure and reactivity similarities and differences between the metal oxo functionality and its corresponding metal hydroxo form will help promote understanding of their complementary roles in oxidation processes and aid in the rational design of selective oxidation catalysts to match different requirements. This review summarizes the structure and reactivity similarities and differences of the reported redox enzymes and their models in which the metal oxo and/or corresponding metal hydroxo moieties have demonstrated their activity in oxidation processes. Those enzymes include heme enzymes, lipoxygenases, sulfite oxidases and xanthine oxidases, because the heme enzymes and lipoxygenases would provide the platform to compare the iron oxo with its corresponding hydroxo species, and the sulfite oxidases and xanthine oxidases provide the platform for molybdenum oxo and hydroxo species.

1. Introduction

Transition metal ions play central roles in a series of biological oxidation events including hydroxylations; epoxidations; dehalogenations; sulfoxidations; dehydrogenations; N, S, and O-dealkylations; alcohol and aldehyde oxidations; and oxidative deaminations and dehalogenations [1,2]. They also play critical roles in the oxidative processes employed in chemical industry and laboratory synthesis. In the presence of a specific ligand, the oxidation properties of the transition metal ion are highly controllable. For example, simple salicylaldimine complexes of manganese (Mn^{III}(salen)'s) can catalyze olefin epoxidations without enantioselectivity, whereas in the presence of asymmetric salen ligands, the Jacobsen–Katsuki catalysts are capable of catalyzing a variety of asymmetric epoxidations with high enantioselectivity [3]. Although the categories of the oxidation reactions may change from substrate to substrate, traditionally, the late transition metal oxo moieties, i.e., M^{n+}=O, have been proposed to serve as key, active intermediates in most oxidation reactions, and an oxygen rebound mechanism coined by Groves has been generally applied to interpret the role of the metal ions in these redox metalloenzymes and synthetic oxidation catalysts [1,4].

While metal oxo moieties are recognized as the key, active intermediates in a wide variety of oxidation processes, there are exceptions. In iron and manganese lipoxygenases, an iron(III) or manganese(III) hydroxo moiety, not the iron(III) or manganese(III) oxo species, has been presumed to serve as the active intermediate for hydrogen abstraction from 1,4-pentadiene containing fatty

* Tel.: +86 27 87543732.
E-mail address: gyin@hust.edu.cn.

0010-8545/$ – see front matter © 2010 Elsevier B.V. All rights reserved.
doi:10.1016/j.ccr.2010.01.016

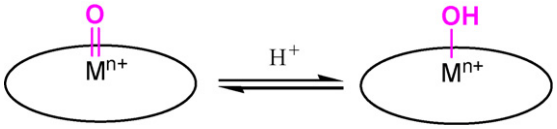

Fig. 1. The metal oxo and its corresponding metal hydroxo form.

acids [5,6]. In xanthine oxidases, the Mo^{VI}–OH group rather than the Mo^{VI}=O group is now accepted as the active functional group for hydroxylation of hypoxanthine [7]. Even among the heme enzymes, Green has recently suggested that the compound II in chloroperoxidases (CPO) is in the iron(IV) hydroxo form rather than the well accepted iron(IV) oxo form [8]. Since high oxidation state transition metal ions participate in so many important biological and chemical oxidation events, there is growing interest in understanding reactivity similarities and differences between oxo and hydroxo intermediates. If reactivity patterns can be recognized in nature's choice between oxo and hydroxo intermediates, it may be possible to apply these structure–function relationships to the rational design of oxidation catalysts. Since the oxo and hydroxo species have the same coordination environment and oxidation state of the metal, the key difference is the protonation state of oxygen which may significantly influence the reactivity of the metal center (Fig. 1).

This review will highlight the similarities and differences in redox reactivity between transition metal oxo species and their corresponding metal hydroxo intermediates in redox enzymes and their models. While the metal oxo forms of iron, molybdenum, vanadium, tungsten and other metalloenzymes have been widely reported as the active intermediates in oxidation events; up to now, only the iron(IV) hydroxo, molybdenum(VI) hydroxo, and iron(III) hydroxo and manganese(III) hydroxo moieties have been reported as alternative intermediates in heme enzymes, xanthine oxidases and lipoxygenases, respectively. Therefore, in this review, the structure and reactivity information from the heme enzymes and their models is highlighted to compare the iron(IV) oxo species with its corresponding iron(IV) hydroxo moiety. Similar information regarding sulfite oxidases, xanthine oxidases and their models is highlighted to compare the molybdenum(VI) oxo species with its corresponding molybdenum(VI) hydroxo moiety. (Because space is limited, the sulfite oxidases have been chosen as representative enzymes with molybdenum(VI) oxo active intermediates.) Information concerning lipoxygenases and their models is also included in this review because the structure and reactivity of the iron(III) hydroxo and manganese(III) hydroxo intermediates in lipoxygenases and their models may also provide useful information for understanding the differences between iron oxo and iron hydroxo intermediates. Finally, synthetic inorganic models are highlighted to provide an overall view of the structure, physical and chemical properties, and reactivity similarities and differences of metal oxo and metal hydroxo active sites.

2. The structures and reactivities of compound I $(porph^{+\bullet})Fe^{IV}$=O and compound II $(porph)Fe^{IV}$=O in heme enzymes and their synthetic models

The heme enzymes, including cytochrome P450 enzymes, peroxidases and catalases, are an important family of redox enzymes which catalyze a wide variety of biochemical oxidation and electron transfer reactions [9–13]. Although the functions of these enzymes are significantly different, their active sites generally have a similar active center comprised of an iron ion with one protoporphyrin ligand and one proximal ligand (Fig. 2). The porphyrin ligand is conserved in all of these heme enzymes, while the proximal ligand is enzyme-dependent. In the cytochrome P450 enzymes, the proximal ligand is a cysteine thiolate group; whereas it is a tyrosine phenolate in the catalases and is a histidine residue in the peroxidases [14]. In the P450 enzymes, the cysteine thiolate ligand facilitates the heterolytic O–O bond cleavage of the ligated peroxide on the iron center. Once the O–O bond cleavage is occurring, the electron density provided by the thiolate may stabilize the iron ion at the high oxidation state [15–19]. Evidence for this comes from the site-directed mutagenesis of histidine-93(F8) in human myoglobin (Mb) to cysteine (H93C Mb) and tyrosine (H93Y Mb) [20]. The redox potentials of the Fe^{3+}/Fe^{2+} couples in the mutants are lower than that observed for wild type Mb. The Fe^{3+}/Fe^{2+} couples are −230 mV in H93C Mb and −190 mV in H93Y Mb, whereas the couple for wild type Mb is +50 mV. The redox potential change in the mutants can be interpreted in terms of stabilizing the ferric heme iron with the negatively charged thiolate from cysteine or phenolate from tyrosine [21–24]. When wild type Mb is treated with cumene hydroperoxide oxidant, the oxidation proceeds by both heterolytic and hemolytic reaction mechanisms to form $(porph^{+\bullet})Fe^{IV}$=O and $(porph)Fe^{IV}O$, respectively. The presence of the thiolate ligand in cysteine (H93C Mb) enhanced heterolytic O–O bond cleavage upon addition of cumene hydroperoxide. The phenolate ligand in tyrosine (H93Y Mb) had no obvious influence on O–O bond cleavage [20].

The sixth coordination site of the iron ion in heme enzymes is an open site for reactions. In the P450 enzymes, it is the site for dioxygen binding, dioxygen activation, O–O bond cleavage, and oxygen atom transfer to the substrate (Fig. 3) [25–27]. During the catalytic cycle, the first active intermediate (compound I) is a ferryl oxo species with a radical delocalized on the porphyrin ring, that is $(porph^{+\bullet})Fe^{IV}$=O. The ferryl oxo–porphyrin cation radical form has become a generally accepted model for compound I in all of the P450 enzymes. Compound I intermediates are also observed for the peroxidases, but the mechanism of formation is different for the two classes of enzymes. In the P450 enzymes, compound I is generated by oxidation of iron(II) through dioxygen binding followed by a series of steps that leads to breaking of the O–O bond as shown in Fig. 3. In the peroxidases, compound I is formed by direct hydrogen peroxide binding to the iron(III) center followed by base-assisted heterolytic cleavage of the O–O bond. The rapid formation and subsequent breakdown of compound I in cytochrome P450 was first experimentally observed by Sligar and coworkers in 2002 [28]. In the reaction of a thermostable P450 with *m*-chloroperoxybenzoic acid (*m*-CPBA) at 4 °C, the resulting intermediate displayed the spectroscopic signature of compound I that has been observed and reported for other heme enzymes [29–32]. The relatively long half-

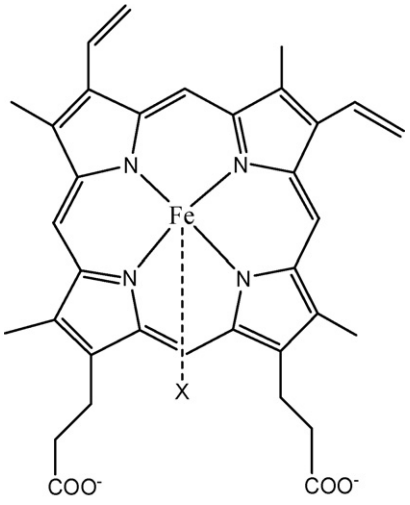

Fig. 2. The macrocyclic ligand structure of the heme enzymes.

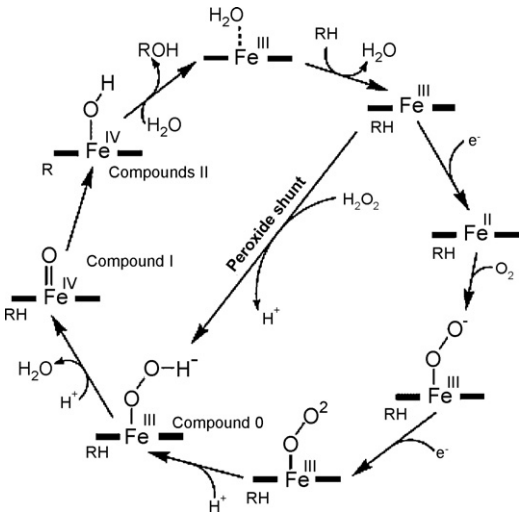

Fig. 3. The catalytic cycle in P450 enzyme.
(Figure was modified from Ref. [27], with permission of the copyright holders.)

life of the compound I generated in this study allowed the authors to investigate the kinetics of its formation and decomposition; the formation of the compound I is a second order process with a rate of 3.20 ($\pm$0.3) $\times$ 10^5 M^{-1} s^{-1} at pH 7.0, 4 °C, while its decomposition is a first order process with a rate of 29.4 $\pm$ 3.4 s^{-1} which is 10^5 times faster than the decomposition of compound I in the catalases [33,34].

Compound I is a highly reactive intermediate in heme enzymes. It can transfer the activated oxygen from the ferryl oxo to the substrate in the peroxygenase cycle, thus reducing itself to iron(III), or it can accept one electron from the substrate to form the second active intermediate, compound II, in the peroxidase cycle (Fig. 4). In peroxidases, compound I generally serves as the oxidant for electron transfer rather than as an oxygen transfer agent, because the protein environment inhibits substrate access to the ferryl oxo functional group. The key finding to support this point comes from the investigations of Ortiz de Montellano and coworkers. Cytochrome P450 can react with phenylhydrazine to produce a relatively stable intermediate, and the X-ray structure of such an intermediate revealed that the phenyl group from phenylhydrazine is directly bonded to the iron center [35–37]. In contrast, no such phenyl-iron intermediate was observed for horseradish peroxidase, lignin peroxidase, manganese peroxidase, or Coprinus macrorhizus peroxidase, implying that the ferryl oxo species in these classical peroxidases are not readily accessible to the substrate [38–40]. Consequently, transfer of one electron from substrate to the active site of these peroxidases reduces compound I to compound II leaving the ferryl oxo group unchanged. To investigate the difference in oxidizing ability between compounds I and II, Yamazaki and coworkers studied the redox properties of compounds I and II in several peroxidases [41–43]. In arthromyces ramosus peroxidase (ARP), compound I can be directly reduced to ferric ARP via titration with ascorbate under neutral pH conditions, while compound II was only observed as an intermediate when the titration was carried out under alkaline pH conditions. Using an EPR spectrometer with a microflow system, the authors also found that the ARP catalyzed oxidation of hydroquinone proceeds by way of a one-electron-transfer mechanism, supporting the idea that compound II was generated by one electron reduction of compound I. The measured redox potentials for compounds I and II in ARP are 0.915 and 0.982 V at pH 7, respectively. The high redox potential of the compound II is also consistent with its unusual instability.

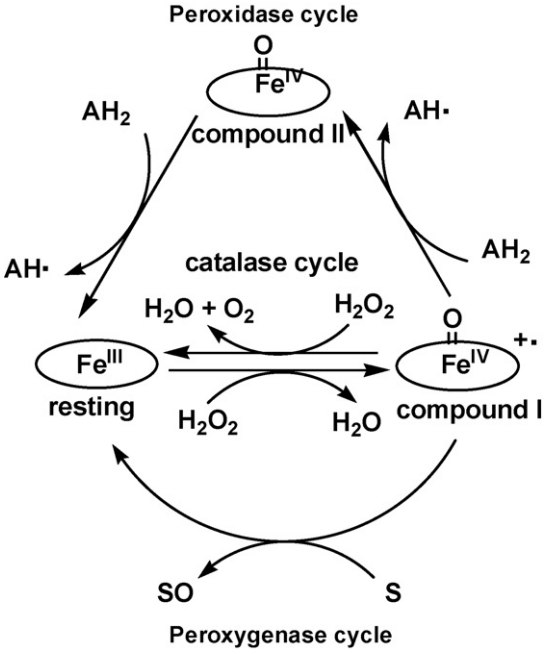

Fig. 4. The roles of the compounds I and II in the catalytic cycles of heme enzymes.

Following discovery of the ferryl oxo form of compounds I and II, the identities of these intermediates have been widely confirmed through preparation of synthetic iron(IV) oxo complexes which are easily generated via oxidation of the corresponding iron(III) porphyrins using chemical oxidants [44–47]. A number of synthetic models containing a metal oxo group have been characterized using UV–visible, EPR, EXAFS, Mössbauer, and NMR spectroscopies, and (in selected cases) by X-ray crystallography [48–57]. An early example is the synthesis of (TMP)Fe^{IV}=O (TMP: tetramesitylporphyrinato) by Groves and coworkers (Fig. 5) [58]. In the first step of this synthesis, wet, basic alumina is used to convert the chloroiron(III) porphyrin to the hydroxoiron(III) complex. The resulting hydroxoiron(III) complex is then treated with $Fe(ClO_4)_3$ to generate first (TMP)$Fe^{III}OClO_3$ and then (TMP$^{+\bullet}$)$Fe^{III}(ClO_4)_2$. Formation of the targeted (TMP)Fe^{IV}=O was achieved through ligand metathesis of (TMP$^{+\bullet}$)$Fe^{III}(ClO_4)_2$ over moist, basic alumina. The kinetics of its formation can be monitored easily by UV–visible spectroscopy because the spectrum of (TMP)Fe^{IV}=O (λ_{max} = 418, 540 nm) is significantly different from that of its precursor (TMP$^{+\bullet}$)Fe^{III} ($C1O_4$)$_2$ (λ_{max} = 395, 505 nm). The (TMP)Fe^{IV}=O species thus generated reacts readily with olefins to afford epoxides at room temperature with some degree of stereochemical control. For example, *cis*-β-methylstyrene can be epoxidized by the active (TMP)Fe^{IV}=O species and the ratio of *cis* to *trans*-epoxide products is highly dependent on the reaction conditions employed. Solutions of (TMP$^{+\bullet}$)Fe^{IV}(O)(Cl), produced by oxidizing chloroiron(III) porphyrin with *m*-CPBA at −78 °C, reacted rapidly with *cis*-β-methylstyrene to give largely the *cis*-epoxide (*cis*/*trans* = 11.3). When the oxidant was generated electrochemically from the hydroxoiron(III) complex in basic solution, *cis*-β-methylstyrene was converted to epoxide with a *cis*/*trans* ratio of 2.3–3.3. When the (TMP)Fe^{IV}=O species was isolated as described in Ref. [58] and then used to epoxidize *cis*-β-methylstyrene the epoxide had a *cis*/*trans* ratio of only 1.0–1.3. Although ferry oxo species were once presumed to be the sole active intermediates in heme-catalyzed olefin epoxidations, recent data suggest that reaction proceeds via multiple, condition-dependent mechanisms [59,60].

Most recently, Collins and coworkers quantitatively generated a deep green [Fe(TAML)O]$^-$ species by oxidation of [PPh_4][Fe^{III}(TAML)(H_2O)] with *m*-CPBA (TAML: tetra-amido macrocyclic ligand) [61]. Through mass spectrometry; Mössbauer, EPR,

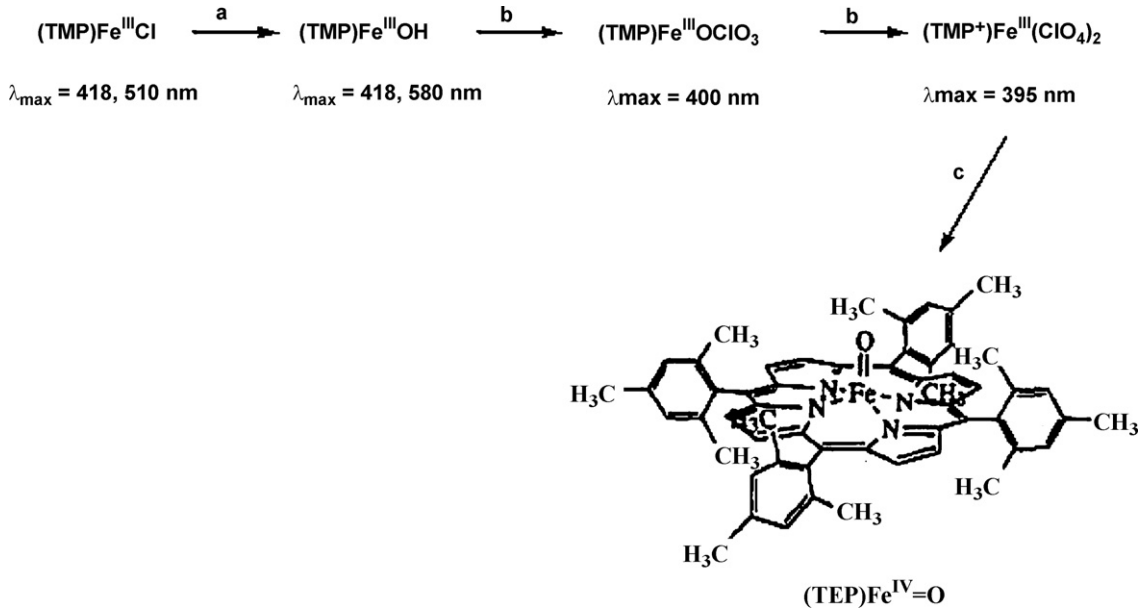

Fig. 5. Synthetic procedure for (TMP)Fe^{IV}=O. (a) CH_2Cl_2, alumina/10% H_2O. (b) CH_2Cl_2, $Fe(ClO_4)_3$. (c) Solutions of **2** in CH_2Cl_2 or benzene filtered through basic alumina/20% H_2O at room temperature.
(Figure was modified from Ref. [58], with permission of the copyright holders.)

and X-ray absorption spectroscopies; as well as reactivity studies and density functional theory calculations, the authors assigned it as a $[Fe^{V}(TAML)O]^{-}$ species. The direct evidence for an iron(V)-oxo unit comes from EXAFS analysis. The Fe–O bond is as short as 1.58 Å, an unusual short distance for a Fe^{IV}–O bond. Consistent with the Fe^{V}=O assignment, $[Fe^{V}(TAML)O]^{-}$ demonstrates the reactivity features of a strongly oxidizing iron-oxo complex. It can quantitatively oxidize triphenylphosphine to the corresponding triphenylphosphine oxide while being reduced to the Fe^{III}(TAML) complex. In the presence of ^{18}O-water, incorporation of ^{18}O into the oxidized product was observed by GC–MS studies. Because there is no evidence of radical delocalized on the TAML ring, the two electron oxidation of the resting Fe^{III}(TAML) is understood to be metal-centered, which is consistent with an iron(V) state rather than an iron(IV) state.

The reactivity of ferryl oxo intermediates has also been investigated extensively in catalytic oxidation processes. Using iodosylbenzene as the oxidant, chloro-α,β,γ,δ-tetraphenyl porphinatoiron(III) can catalyze alkane hydroxylations and olefin epoxidations [62]. When oxidant is added to chloro-α,β,γ,δ-tetraphenylporphinatoiron(III), the active intermediate generated *in situ* is capable of abstracting hydrogen from the robust cyclohexane to form cyclohexanol and of epoxidizing *cis*-stilbene to the corresponding *cis*-stilbene oxide, whereas *trans*-stilbene is an inert substrate. Using a mixture of *cis* and *trans*-stilbene substrate led to efficient isolation of *cis*-stilbene oxide product and unchanged *trans*-stilbene. When using chlorodimethylferriprotoporphyrin as the catalyst, epoxidation of a mixture of *cis* and *trans*-stilbenes afforded the corresponding *cis* and *trans*-epoxides. The authors hypothesize that the dramatic reactivity differences between the two substituted iron porphyrin catalysts arise because of phenyl–phenyl interactions between the stilbene substrates and the phenyl substituents of activated chloro-α,β,γ,δ-tetraphenylporphinatoiron(III). An examination of space filling models suggested that the C=C double bond of the *cis*-stilbene can access the active site without interference, whereas strong phenyl–phenyl non-bonding interactions between catalyst and substrate inhibit the approach of *trans*-stilbene to the active site. One of the most attractive features of the P450 enzymes is that they may regio- and stereospecifically hydroxylate alkanes to the corresponding alcohols [10,63,64]. Groves and coworkers studied the asymmetric hydroxylation of ethyl benzene using a chiral binaphthyl iron porphyrin catalyst to mimic enzyme-mediated asymmetric oxidation [65]. Reaction was carried out in dichloromethane at 0 °C using iodosylbenzene as oxidant (Fig. 6). Hydroxylation of ethylbenzene gave a 40% yield of 1-phenylethanol with a 79:21 ratio of R to S enantiomers. Detailed hydroxylation studies using deuterated ethylbenzene revealed that removal of the *pro*-R hydrogen is twice as likely as removal of the *pro*-S hydrogen.

The generally accepted oxidation mechanism mediated by P450 enzymes and their models is the oxygen rebound mechanism described by Groves, in which the key active intermediate is a high oxidation state ferryl oxo intermediate [4]. Oxygen rebound mechanism in oxygen atom transfer reactions is illustrated in Fig. 7. In the first two steps, the reduced form of the iron center is oxidized to

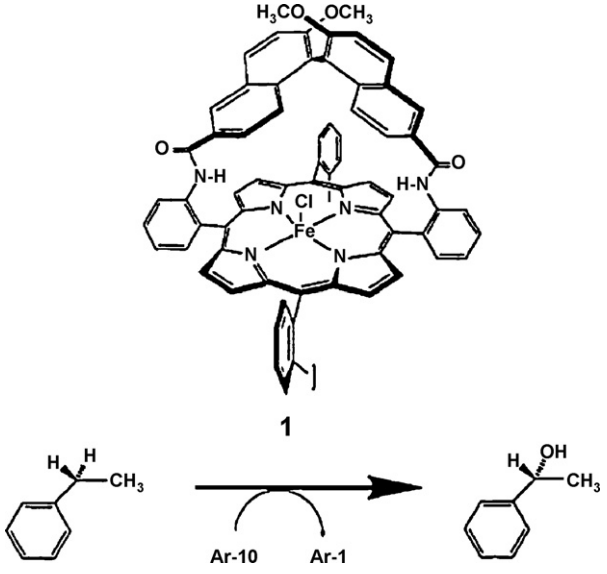

Fig. 6. Asymmetric hydroxylation of ethylbenzene by a chiral iron complex.
(Figure was reproduced from Ref. [65], with permission of the copyright holders.)

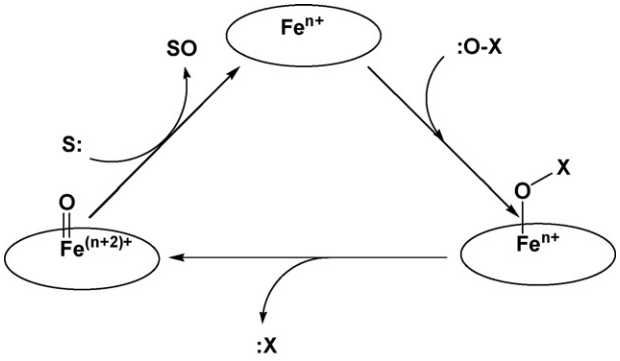

Fig. 7. Oxygen rebound mechanism coined by Groves.
(Figure was modified from Ref. [4], with permission of the copyright holders.)

produce the ferryl oxo species. Next, the ferryl oxo species transfers its activated oxygen to the substrate by oxygenation.

Alternatively, a high valent iron-oxo intermediate abstracts a hydrogen atom from the substrate to form a ferryl hydroxo intermediate which later rebinds with the substrate radical. The experimental evidence to support the oxygen atom transfer mechanism comes from manganese porphyrin catalyzed olefin epoxidations that were carried out independently by Meunier and Groves [66,67]. These definitive experiments that established a Mn^{V}=O species as the active intermediate in olefin epoxidation involved the use of isotopically labeled oxygen—first to confirm oxygen exchange between the manganese oxo species and labeled aqueous solvent ($H_2{}^{18}O$), and then to identify the Mn^{V}=O group as the source of the ^{18}O that was subsequently transferred to the olefin, forming the epoxide-^{18}O (Fig. 8). In addition to the ferryl oxo and Mn(V)=O species, other high oxidation state, late transition metal oxo species including Cr(V)=O, Ru(VI)=O and Re(VII)=O, etc., have been suggested as key active intermediates in oxidation processes [66,68–72].

Although a ferryl hydroxo intermediate (Fe^{IV}–OH, a protonated ferryl oxo group) has been proposed in the oxygen rebound mechanism for alkane hydroxylation [4], neither the ferryl hydroxo form of compound I nor compound II had been proposed for the heme enzymes or their synthetic analogues until quite recently. In 2004, using X-ray absorption spectroscopy, it was shown that the Fe–O bond (1.82 Å) in chloroperoxidase compound II (CPO-II) is much longer than expected for an iron(IV) oxo unit (~1.63 Å) [73]. Using Mössbauer spectroscopy and density functional calculations, the authors determined that the ferryl forms of $P450_{BM3}$ and $P450_{cam}$ are protonated at physiological pH [74]. The experimentally determined Fe–O bond length (1.82 Å) for the CPO-II agrees well with density functional calculations for a protonated ferryl species (Fe^{IV}–OH), whereas the reported ferry oxo (Fe^{IV}–O) distances in horseradish peroxidase compound I (HRP-I) and compound II (HRP-II) are 1.64 Å. In order to minimize the effects of instrumental error in comparing the Fe–O bond lengths in CPO-II, HRP-I, and HRP-II, the authors of the CPO study determined the Fe–O distances in both HRP-I and HRP-II by EXAFS. The bond lengths obtained were in good agreement with those already reported in the literature. Later, Green and coworkers further reported a Fe–O distance of 1.65 Å for CPO-I, which is significantly shorter than that observed for the compound II [75] thus supporting that CPO-I is an authentic ferryl oxo species. This bond length is also in excellent agreement with the value obtained (1.654 Å) from a Badger's rule analysis of the CPO-I ferryl moiety (υ_{Fe-O} = 790 cm^{-1}) [76]. Direct evidence for the iron(IV) hydroxo form of the CPO-II was obtained from the resonance Raman studies of the CPO-II which revealed a ^{2}H and ^{18}O sensitive band at υ_{Fe-O} = 565 cm^{-1} (Fig. 9) [77]. Preparation of CPO-II in H_2O using the ^{18}O-labeled oxidant $H_2{}^{18}O_2$ leads to a red shift of 22 cm^{-1}, while a less dramatic red shift to 552 cm^{-1} is observed when the CPO is oxidized using H_2O_2 in D_2O. These shifts are in good agreement with the isotopic shifts expected for a Fe^{IV}–OH harmonic oscillator (12 and 23 cm^{-1}), leading to the conclusion that the active form of iron in CPO-I is Fe^{IV}=O while the active form of iron in CPO-II is Fe^{IV}–OH.

Recent X-ray structural data also suggest that the Fe–O bond distances in the compound II of HRP, Mb, cytochrome c peroxidase (CCP), and catalase (CAT) are longer than what is expected for a ferryl oxo form. Gerglund and coworkers described a strategy to obtain high resolution crystal structures of the intermediates in HRP at pH 6.5. The Fe–O distance obtained for HRP-II was 1.80 Å which is 0.14 Å longer than that of HRP-I (1.66 Å) [78]. Therefore, the authors argued that the long Fe–O distance supports the assignment of the compound II as an iron(IV) hydroxo species. The authors further hypothesized that the proton of the iron(IV) hydroxo moiety was transferred from the nearby histidine via the intervening water molecule.

The results of these structural studies are, however, in disagreement with earlier studies based on resonance Raman and EXAFS spectroscopy. Using EXAFS, Penner-Hahn and coworkers determined the structural environments of the active sites in HRP-I, HRP-II, and their iron porphyrin analogues [79]. The HRP-I was prepared by the addition of ethyl hydroperoxide to ferric HRP, giving

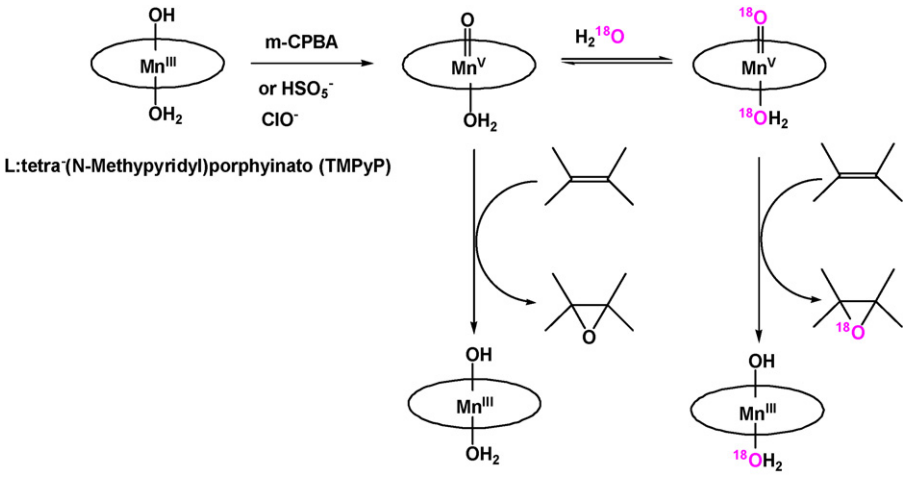

Fig. 8. The isotopically experimental evidence for oxygen rebound mechanism.
(Figure was modified from Ref. [67], with permission of the copyright holders.)

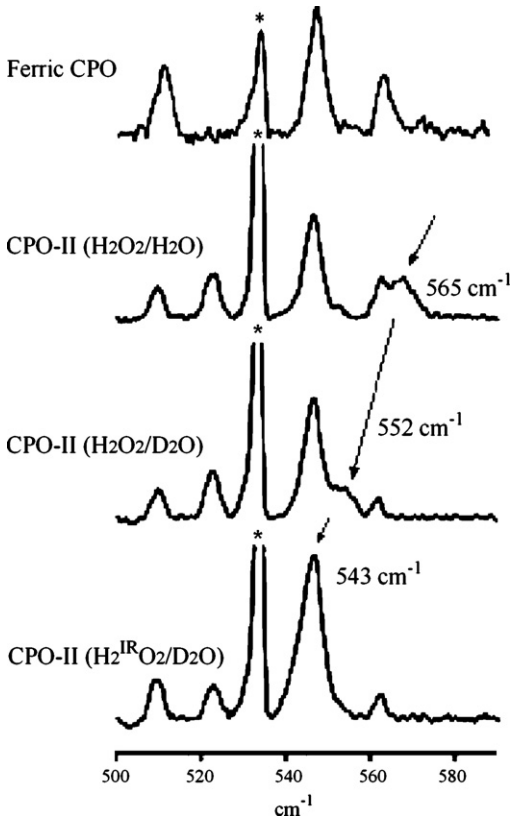

Fig. 9. Low-frequency resonance Raman spectrum of the CPO and CPO-II samples at pH 6.5.
(Figure was modified from Ref. [77], with permission of the copyright holders.)

a characteristic green species of HPR-I. Adding one equivalent of reductant to the resulting HRP-I led to the formation of a red solution, characteristic of HRP-II. The EXAFS spectra of HRP-I and II are identical, and the Fe–O bond distances determined for both HRP-I and II are 1.60 ± 0.3 Å. Application of Budger's rule to this distance affords an Fe–O stretching frequency of 817 cm^{-1} which is consistent with Terner's resonance Raman observation of 787 cm^{-1} for HRP II [80]. In addition, Green's EXAFS measurement also gave a Fe–O distance of 1.70 Å in HRP-II [73]. After reviewing the results from EXAFS, resonance Raman and X-ray crystallography, Green suggested that the ferryl form of HRP-II is not basic ($pK_a \leq 4$), and argued that the long Fe–O distance from the crystal structure either has systematic errors of 0.2 Å or that the active center was photoreduced during the structural determination [81].

Using EPR and ENDOR spectroscopies, Dawson and coworkers recently investigated the cryoreduction of the EPR-silent compound II of various peroxidases to the corresponding iron(III) species by γ-irradiation at 77 K [82]. At this low temperature, the one electron reduction of the iron(IV) ion to the corresponding iron(III) ion was expected to proceed with retention of the iron(IV) precursor's structure. The frozen protein environment would prevent structural/bonding changes even though a redox change was occurring. Thus, the cryoreduction of a $[Fe^{IV}{=}O]^{2+}$ heme would be expected to generate a $[Fe^{III}{-}O]^{+}$ heme, whereas a $[Fe^{IV}{-}OH]^{2+}$ heme would afford a $[Fe^{III}{-}OH]^{+}$ heme. Through EPR and ENDOR studies of the iron(III) heme from cryoreduced HRP-II and CPO-II, it is evident that HRP-II is in a ferryl oxo form and CPO-II is in an iron(IV) hydroxo form, consistent with the results from the EXAFS and resonance Raman studies.

Although the detailed mechanisms for most heme enzyme-mediated oxidation processes remain ambiguous, the ferryl oxo form of compound I has been well accepted. In contrast, recent evidence suggests that the form of compound II is highly enzyme dependent. In chloroperoxidase, the latest data clearly suggest an iron hydroxo form of compound II, whereas for most other peroxidases, the literature contains contradictory observations. Having otherwise identical coordination environments, the key difference between ferryl oxo and ferryl hydroxo moieties is the protonation state which is modulated by the protein environment to facilitate the specific oxidation events in enzymes. However, the ambiguous protonation state of compound II in most peroxidases makes it difficult to fully understand the mechanisms of reactions mediated by those peroxidases. Clarifying the reactivity similarities and differences of the ferryl oxo and its corresponding ferryl hydroxo form would apparently help to understand their roles in oxidation events in heme enzymes, thus promote understanding their mechanisms.

3. Metal–oxygen intermediates of sulfite oxidases and their synthetic models

Molybdenum is involved in more than 30 enzymes which mediate two electron oxidation processes that are critical for the metabolism of C, N, and S by all forms of life [7,9]. Among these molybdenum enzymes, the sulfite oxidases catalyze oxidation of sulfite to sulfate, the final step in the degradation of sulfur containing compounds like cysteine. Sulfite oxidase is a dimeric enzyme, and each monomer contains one molybdenum active center which is associated with a cytochrome heme. The oxidation of sulfite occurs at the molybdenum site, and the cytochrome heme serves to re-oxidize the reduced molybdenum ion through electron transfer. In the crystal structure of chicken liver sulfite oxidase, the molybdenum atom has square pyramidal geometry, coordinating with three sulfur atoms and two terminal oxo ligands (Fig. 10) [83]. All three coordinated sulfur atoms are located in the equatorial plane; two are from the dithiolene group of molybdopterin and the third is part of a cysteine side chain. The active functional group at the molybdenum site is believed to be the oxo group in the equatorial plane. Access of the sulfite substrate to the other (axial) oxo ligand is blocked by the protein environment. The catalytic cycle of sulfite oxidase begins with the two electron oxidation of sulfite to sulfate at the molybdenum center. The combined evidence from model studies, ^{18}O labeling experiments, and stopped-flow investigations supports that oxidation of sulfite occurs by oxygen transfer from $Mo^{VI}{=}O$ to sulfite, resulting in a reduced Mo^{IV} form [7,84,85]. Re-oxidation of the Mo^{IV} ion to the active Mo^{VI} ion by the nearby Fe^{III} ion occurs through two independent intramolecular electron transfers (IET). A Tyr^{322} residue was hypothesized to mediate proton coupled electron transfer from Mo^{VI} to Fe^{III}. The re-oxidation of Fe^{II} ion to Fe^{III} is accomplished by one-electron transfer to exogenous cytochrome c (Fig. 11) [86–88]. By investigating the intramolecular electron transfer between $Mo^{VI}Fe^{II}$ and $Mo^{V}Fe^{III}$ forms of chicken liver sulfite oxidase, Enemark and coworkers found that intramolecular electron transfer from Mo^{V} ion to Fe^{III} ion is coupled with proton transfer from $Mo^{V}{-}OH$ to OH^{-}, whereas the reverse intramolecular electron transfer process is coupled with the proton transfer from H_2O to $Mo^{VI}{=}O$. Furthermore, when small anions like SO_4^{2-} or Cl^{-} blocked the approach of H_2O or OH^{-} to the Mo–OH center, the nearby Tyr^{322} was thought to play an important intermediary role in proton transfer [89].

Of the three coordinated sulfur atoms associated with the molybdenum center, the dithiolene group of molybdopterin is conserved in most monomeric molybdenum enzymes. Its role in sulfite oxidation has received considerable attention. High oxidation state early transition metal ions like Mo^{VI} have relatively poor oxidizing power. While direct oxygen transfer from a $Mo^{VI}{=}O$ functional group to an easily oxidizable substrate such as PPh_3 may be possible, an additional mediator is essential to facilitate oxygen transfer

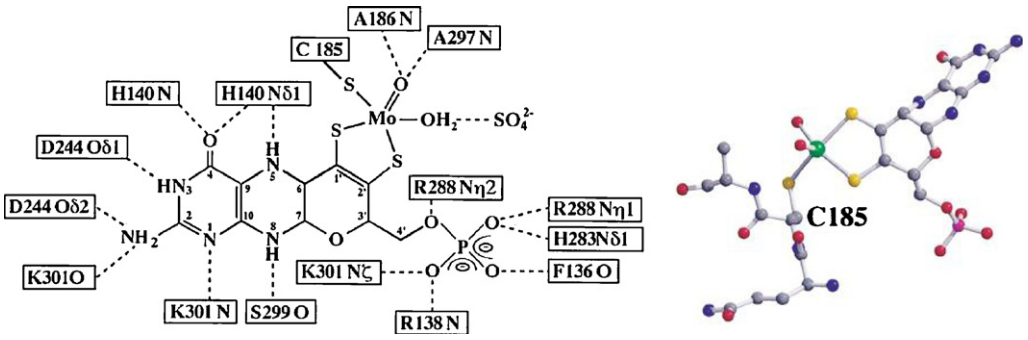

Fig. 10. The coordination environment of molybdenum and its anchoring by molybdopterin in the active site of chicken liver sulfite oxidase. (Figure was modified from Ref. [83], with permission of the copyright holders.)

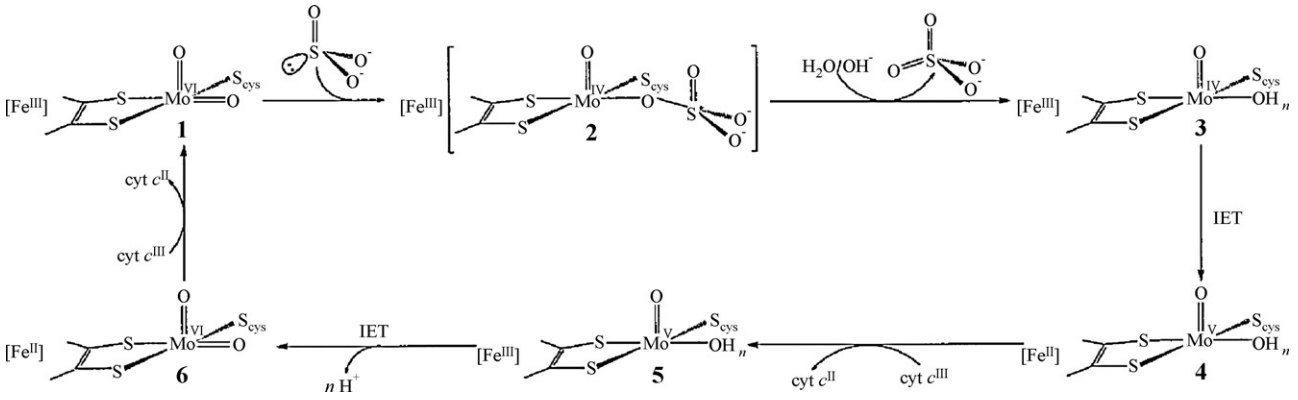

Fig. 11. Proposed oxidation reaction mechanism for the sulfite oxidase. (Figure was reproduced from Ref. [86], with permission of the copyright holders.)

from Mo^{VI}=O to oxidize substrates such as sulfite. Accordingly, the dithiolate ligand has been suspected to play a critical role in modulating the redox potential of the molybdenum to facilitate both oxygen transfer from Mo^{VI}=O to the substrate and re-oxidation of the Mo^{IV} ion to the Mo^{VI} ion [90–93].

A number of synthetic, molybdenum model complexes containing two or more sulfur ligands have been prepared and some of them were tested as oxygen transfer catalysts. For example, Holm and coworkers demonstrated oxygen transfer between a synthetic Mo(VI) complex and a triaryl phosphine substrate (Fig. 12) [94]. In DMF solution, the synthetic $Mo^{VI}O_2$(L-NS_2) complex (L-NS_2 = 2,6-bis(2,2-diphenyl-2-mercaptoethyl)pyridine) can transfer oxygen from the Mo^{VI}=O unit to $(p\text{-}FC_6H_4)_3P$ as it is reduced back to the Mo^{IV} form. The reduced Mo^{IV} ion can be re-oxidized by N-oxide or sulfoxide through oxygen transfer. As an example of its oxygen transfer capabilities, this molybdenum complex facilitated catalytic oxygen transfer from N-oxide to triarylphosphine with over 100 turnovers in 15 h. Very interestingly, the measured activation entropy for oxygen transfer from $Mo^{VI}O_2$(L-NS_2) to triphenylphosphine is about −28.4(1.6) eu, whereas the activation entropies are +7.2(2.0) and +2.6(1.6) eu for oxygen transfer from N-oxide and S-oxide to the reduced Mo^{IV}O (L-NS_2), respectively.

Sarkar and coworkers prepared three bis(dithiolene) containing molybdenum complexes with Mo in the +4, +5 and +6 oxidation states $[Bu_4N]_2[Mo^{VI}O_2(mnt)_2]$, $[Bu_4N]_2[Mo^{IV}O(mnt)_2]$, and $[Ph_3PNPPh_3][Et_4N][Mo^{V}OCl(mnt)_2]$ (mnt^{2-} = 1,2-dicyanoethylenedithiolate) which represent the three oxidation states of molybdenum in sulfite oxidases [95,96]. The structure of the PBu_4^+ salt of the $[Mo^{VI}O_2(mnt)_2]^{2-}$ anion was determined by X-ray crystallography (Fig. 13). This synthetic molybdenum(VI) complex has a distorted octahedral geometry with the two oxo groups arranged *cis* to one another. This molybdenum(VI) dioxo complex is capable of transferring one oxygen to the biological important substrate sulfite, resulting in the reduced molybdenum(IV) monooxo complex and sulfate. However, the molybdenum(V) intermediate was not observed during the oxygen transfer. Additional studies revealed that ions structurally similar to sulfite, including SO_4^{2-}, $H_2PO_3^-$ and $H_2PO_4^-$, prevent oxo transfer from the Mo^{VI}=O group to sulfite because of their competitive coordination. This is the first example of competitive inhibition relevant to the native sulfite oxidases [89]. Using the same $[Mo^{VI}O_2(mnt)_2]^{2-}$ complex,

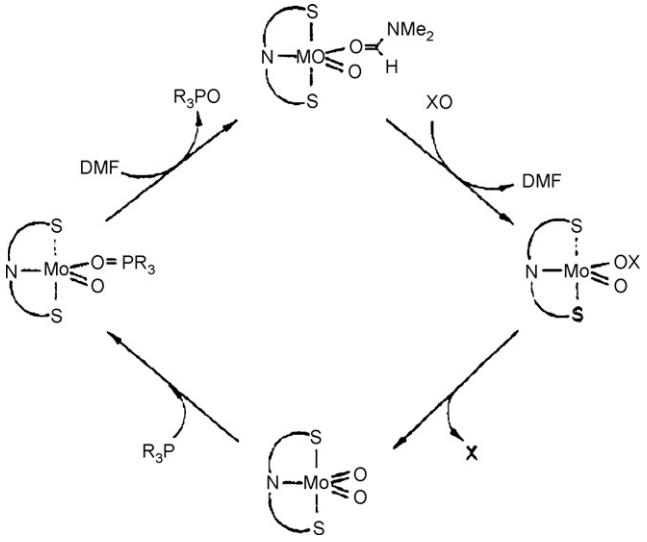

Fig. 12. Catalytic oxygen transfer by molybdenum complex. (Figure was modified from Ref. [94], with permission of the copyright holders.)

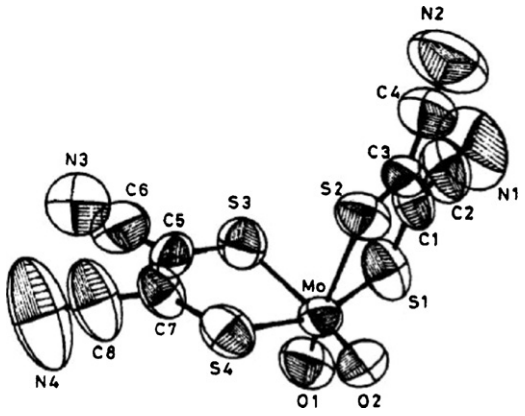

Fig. 13. The X-ray structure of the $[Mo^{IV}O_2(mnt)_2]$ anion in $[Bu_4P]_2[MO^{VI}O_2(mnt)_2]$. (Figure was reproduced from Ref. [95], with permission of the copyright holders.)

Nordlander and coworkers investigated the influence of both the basicity and the steric hindrance of the oxo acceptor on the oxygen transfer process. In oxygenation of $PPh_{3-x}Et_x$ ($x = 0$–3), the reactivity increased linearly with the basicity of the substrate in the order $PEt_3 > PEt_2Ph > PEtPh_2 > PPh_3$. The steric bulk of substituents on the substrate does not exercise a significant influence on oxygen transfer, suggesting that the entering substrate binds to the Mo(VI) center through the oxo group. This is fully consistent with the reaction proceeding via phosphine attacking an oxo ligand rather than coordinating directly to the molybdenum center [97].

In most synthetic models of sulfite oxidase, thiolate ligands occupy two or four sites in the coordination sphere of the molybdenum center rather than the three sites they occupy in natural sulfite oxidases (one from the cysteine side chain and two from the dithiolate group of molybdopterin) [7,9]. The *cis*,*trans*-(L-N_2S_2)Mo^VO(SR) complexes (L-$N_2S_2H_2$: N,N′-dimethyl-N,N′-bis(mercaptophenyl)ethylenediamine; R: CH_2-Ph, CH_2CH_3, and *p*-C_6H_4-Y (Y: CF_3, Cl, Br, F, H, CH_3, CH_2CH_3, and OCH_3)) developed by Enemark and coworkers are the first well characterized monomeric molybdenum(V) complexes having three thiolate ligands similar to the active center of the sulfite oxidases (Fig. 14) [98]. Furthermore, X-ray analysis reveals that these molybdenum(V) models are structurally similar to the molybdenum center in sulfite oxidase. For example, all three of the sulfur atoms are located in the equatorial plane. This coordination geometry places two adjacent sulfur p_π orbitals parallel to the Mo=O bond in a manner analogous to that observed for the molybdopterin in sulfite oxidases

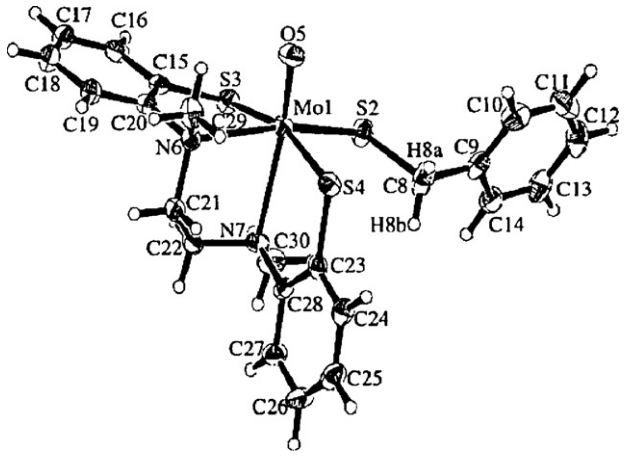

Fig. 14. ORTEP of *cis*,*trans*-(L-N_2S_2)$Mo^VO(SCH_2Ph)$. (Figure was reproduced from Ref. [98], with permission of the copyright holders.)

(Fig. 10). Compared to the spectra of older model complexes having two or four sulfur atom ligands, the EPR spectra of these *cis*,*trans*-(L-N_2S_2)Mo^VO(SR) complexes are quite similar to those of the natural sulfite oxidases.

4. Metal–oxygen intermediates of xanthine oxidases and their synthetic models

The xanthine oxidases, which catalyze hydroxylation of the C–H bond at the 8-position of hypoxanthine and the subsequent hydroxylation of xanthine to uric acid, are the most studied molybdenum enzymes. The xanthine oxidase active site has the general structure $LMo^{VI}(O)(S)(OH)$, where L represents the dithiolene group of molybdopterin common to all mononuclear molybdenum enzymes [7,9]. Although it is known that the oxygen incorporated into the products by xanthine oxidases originates from the solvent, water, early studies looking at a single turnover showed that it comes proximally from the catalytically labile oxygen on the molybdenum center [99]. In addition, synthetic molybdenum(VI) models with a Mo^{VI}=O group transfer oxygen from Mo^{VI}=O to substrates such as triphenylphosphine [100–102]. Because the active site of the xanthine oxidases has a Mo^{VI}=O group, this group was hypothesized to be the oxygen source for hydroxylation of substrate. Hydroxylation is described to proceed by deprotonation of the 8-position carbon of the substrate resulting in a carbanion which attacks on the electron deficient Mo^{VI}=O group to form the Mo(O)(SH)(OR) intermediate (Fig. 15). More recent observations provide an alternative explanation. Wedd and coworkers' studies of the ^{17}O hyperfine EPR coupling signals from the Mo^V ion in xanthine oxidase suggest that the catalytically labile oxygen for hydroxylation originates from a Mo^{VI}–OH group rather than the commonly supposed Mo^{VI}=O group [103]. A similar hypothesis was also put forward by Bray and coworkers [104]. Through detailed studies of the exchange of ^{17}O from labeled solvent into the molybdenum center of xanthine oxidase during a single turnover, Hille and coworkers found that after an initial hydroxylation event, the ^{17}O is incorporated into the molybdenum center at a strongly coupled site ($a_{av} \sim 7$ G) [105]. In a model compound, the Mo–OH group couples strongly to the unpaired electron spin ($a_{av} \sim 6.5$ G), whereas the Mo=O group couples much more weakly ($a_{av} \sim 2$ G) [103]. Thus, Hille suggested that the catalytically labile group in the molybdenum center is the Mo^{VI}–OH group rather than the Mo^{VI}=O group.

For the hydroxylation of substrate by Mo^{VI}–OH in xanthine oxidases, the evidence does not support the oxygen rebound mechanism [4]. The preferred mechanism is one in which an active site base (presumed to be the conserved glutamate residue) abstracts the proton from the Mo^{VI}–OH functional group to initialize nucleophilic attack of the oxygen atom on the 8-position carbon of hypoxanthine, while the hydride from the same carbon transfers to Mo^{VI}=S (Fig. 16). Using a sluggish substrate, Nishino and coworkers obtained a crystal structure of the key intermediate: a carbon oxygen bond has formed, the Mo^{VI}=S group has been protonated to form Mo^{IV}–SH, and the product remains coordinated to the molybdenum center [106]. Evidence for a two-electron hydride transfer rather than two discrete one electron steps comes from the observation that there is no clear correlation between the kinetic parameters of hydroxylation and the redox potentials of the substrates. If the reaction proceeded by sequential one electron steps, the hydroxylation rates of purines would inversely correlate with redox potentials for the one electron $S^{+\bullet}/S$ couples of the heterocycles. The observed kinetic data are inconsistent with sequential one-electron transfer processes [107–109]. In addition, electronic structure investigations of the *cis*-Mo(O)(S) unit also supported a two-electron hydride transfer [110,111].

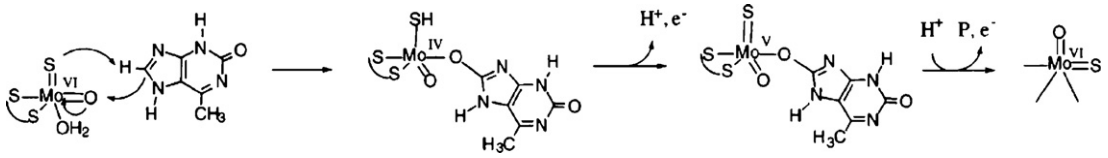

Fig. 15. The early hydroxylation mechanism by xanthine oxidases.
(Figure was reproduced from Ref. [7], with permission of the copyright holders.)

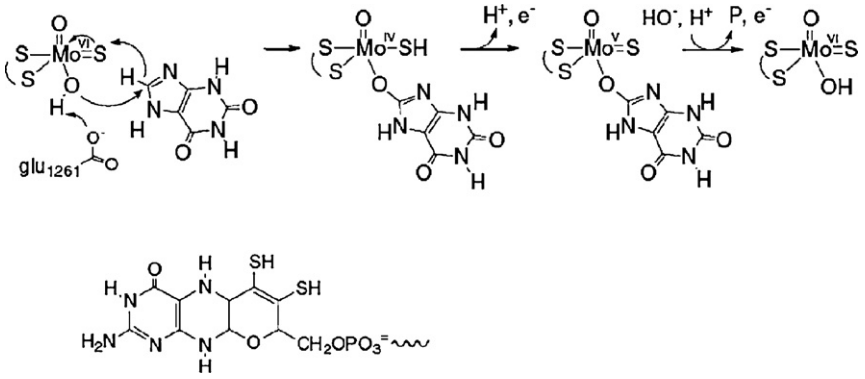

Fig. 16. Proposed base-assisted hydroxylation mechanism for xanthine oxidase.
(Figure was modified from Ref. [107], with permission of the copyright holders.)

The role of the dithiolene group of molybdopterin during the hydroxylation of hypoxanthine remains ambiguous just as it is for the sulfite oxidases. Because this cofactor is a conserved ligand that provides two donor sulfur atoms in most monomeric molybdenum enzymes, its importance is undoubted. In the case of the hydroxylases, Hille suggested two roles it may play. One is to anchor the molybdenum atom at the correct position in the protein, since the polypeptide itself does not ligate the molybdenum atom; another is to modify the redox potential of the molybdenum ion during substrate hydroxylation much as it has been presumed to do in the sulfite oxidases. In the oxidized form of the enzyme, a partial disulfide bond is formed to provide electron density to the Mo^{VI} center, causing its reduction potential to become more negative. In addition, formation of a partial disulfide bond may also help to stabilize the five-coordinate molybdenum(VI) center [90–93,112,113].

Since the active site of the xanthine oxidase contains one oxo, one sulfido, one hydroxo/water, and one dithiolene group, incorporation of all of these functional groups in one model remains a challenge. Holm and coworkers synthesized and thoroughly characterized a series of *cis*-$Mo^{VI}(O)_2L$ and *cis*-$Mo^{VI}(O)(S)L$ complxes (L = Me_4Phen), and their tungsten analogues. Very interestingly, when the *cis*-$Mo^{VI}(O)(S)(OSiPh_3)(Me_4phen)$ complex is treated with PPh_3 in CD_2Cl_2 solution, the ^{31}P NMR spectrum demonstrated that the sulfido group rather than the oxo group was transferred from the Mo^{VI} center to PPh_3 to form a $SPPh_3$ product; no $OPPh_3$ product was detected. Transfer of the sulfur atom rather than the oxygen atom was interpreted in terms of the Mo^{VI}=S bond energies being lower than those of the Mo^{VI}=O group (Fig. 17) [114]. The tungsten analogues of $Mo^{VI}(O)_2(S)L$ and $Mo^{VI}(O)(S)_2L$, which are the most accurate models of the xanthine oxidases produced to date, have also recently been isolated by Holm and coworkers (Fig. 18) [115]. Because the monomeric Mo^{VI} center with two oxo ligands and one sulfido ligand is unstable, the tungsten was applied to stabilize the M^{VI} state. The $W^{VI}(O)_2(S)L$ analogue was synthesized by treating $(Et_4N)_2[WO_3(bdt)]$ (bdt = benzene-1,2-dithiolate) with H_2S at low temperature, and an X-ray crystal structure revealed that the $W^{VI}(O)_2(S)L$ analogue has a distorted square pyramidal geometry similar to that of the xanthine oxidases. Most notably, it has an apical oxo ligand and a basal sulfide ligand.

5. The structure and the related function of the lipoxygenases: metal–hydroxy intermediates as competent oxidants

Lipoxygenases are a family of mononuclear non-heme iron enzymes which catalyze the regio- and stereospecific dioxygenation of 1,4-Z,Z-pentadiene containing fatty acids to alkyl hydroperoxides [116]. The active site of the lipoxygenases contains a ferric/ferrous ion, and the crystal structures of two plant lipoxygenases, soybean lipoxygenase-1 (SLO-1) and soybean lipoxygenase-3 (SLO-3), are known [117–120]. The crystal structure of resting ferrous SLO-1 shows that the reduced iron(II) ion is coordinated to six ligands including three histidines (His499, His504 and His 699), one C-terminal carboxylate from Ile839,

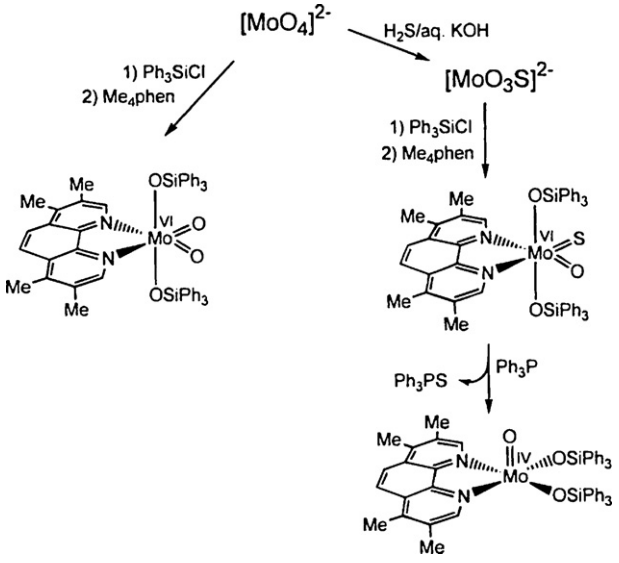

Fig. 17. Preparation of *cis*-$Mo^{VI}(O)_2L$ and *cis*-$Mo^{VI}(O)(S)L$ complexes (L = Me_4Phen) and the related sulfido transfer reactions.
(Figure was reproduced from Ref. [114], with permission of the copyright holders.)

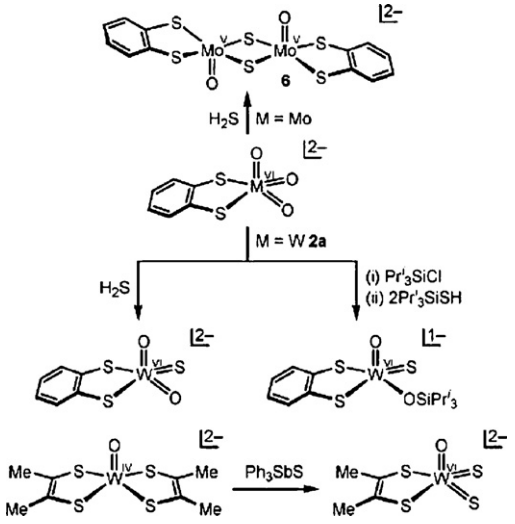

Fig. 18. The synthetic procedures to the tungsten analogues of the $Mo^{VI}(O)_2(S)L$ and $Mo^{VI}(O)(S)_2L$ and the Mo^{V} dimmer model.
(Figure was modified from Ref. [115], with permission of the copyright holders.)

one distant side chain carbonyl of Asn694, and one water (Fig. 19).

All three histidine residues, the carboxylate from isoleucine, and the asparagine residue are conserved in all of the sequenced lipoxygenases with the exceptions that valine replaces isoleucine in rat leukocyte 5-LO and a histidine occupies the position of asparagine in rabbit reticulocyte and human 15-LOs [121,122]. Using circular dichroism (CD) and magnetic circular dichroism (MCD). The resting ferrous site is actually a mixture of five-coordinate and six-coordinate species in a ratio of 40/60 [123]; and, in the presence of coordinating ligand like glycerol, it becomes completely six-coordinate.

Unlike the iron(IV) oxo group that serves as the key active intermediate in heme enzymes, the active intermediate in the lipoxygenases is an iron(III) hydroxo group, Fe^{III}–OH, which plays a key role in abstracting hydrogen from the 1,4-Z,Z-pentadiene containing fatty acids. The iron(III) oxo form of the active intermediate, Fe^{III}=O, was never proposed. Without the π-electron system that serves to stabilize the high valent iron(IV) ion in the porphyrins, the three histidine donors in the lipoxygenases may only be capable of stabilizing iron in the +3 oxidation state. The hydrogen abstraction mediated by the iron(III) hydroxo group is highly regio- and stereospecific in lipoxygenases. For example, in investigating the regio- and stereochemical steps in the oxygenation of 8,11,14-eicosatrienoic acid by SLO-1, it was shown that the *Pro*-S hydrogen was stereospecifically abstracted from C-13 and

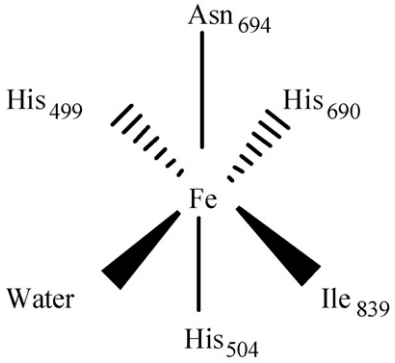

Fig. 19. Active site of wild type soybean lipoxyganse-1.

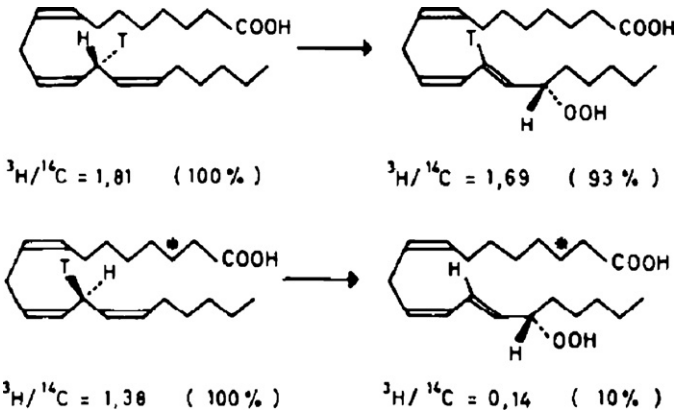

Fig. 20. The stereospecific hydrogen abstraction by lipoxygenase demonstrated by isotopically labelling experiments.
(Figure was modified from Ref. [125], with permission of the copyright holders.)

dioxygen was regio- and stereospecifically inserted at the C-15 to produce a (15S)-hydroperoxide (Fig. 20) [124,125]. In the catalytic cycle, the reduced Fe^{II}–OH_2 species can be re-oxidized to the active Fe^{III}–OH species by the alkyl peroxyl radical (Fig. 21) [120]. The formation of the alkyl peroxyl radical was also confirmed by Fukuzumi through EPR observations [126]. In the hydrogen abstraction step, large kinetic isotopic effects (KIE) have been reported for SLO-1 (KIE ~ 80) and human 15-LO-1 (KIE ~ 50), suggesting that hydrogen abstraction is the rate determining step for the whole catalytic cycle. However, detailed studies also revealed that the abnormally large isotope effect may not originate from a single hydrogen abstraction step, but could instead be the result of multiplicative terms in a reaction that has more than one isotopically sensitive step and may involve reaction branching [127–132].

In consideration of the relatively weak hydrogen abstraction capability of an iron(III) ion, the driving force for hydrogen abstraction originates in part from the coordinative flexibility of the iron center. As described above, the resting, ferrous form is six-coordinate and includes a distance side chain carbonyl donor from the Asn694. In contrast, the ferric form is five coordinate and lacks the carbonyl ligand [123]. Density functional theory calculations also suggest that the coordinative flexibility of the iron center helps

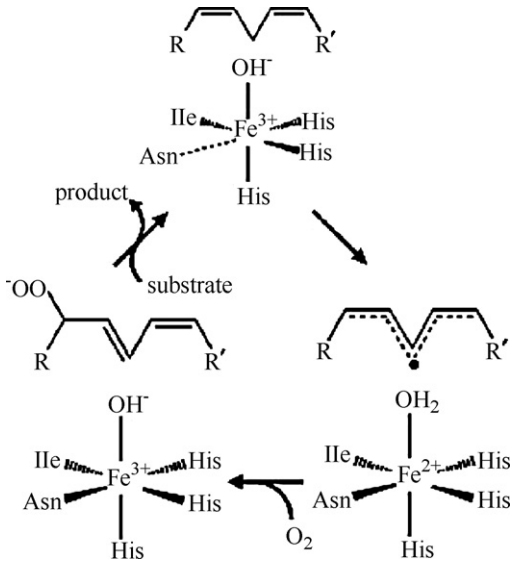

Fig. 21. Proposed hydrogen abstraction mechanism for soybean lipoxygenase-1.
(Figure was modified from Ref. [120], with permission of the copyright holders.)

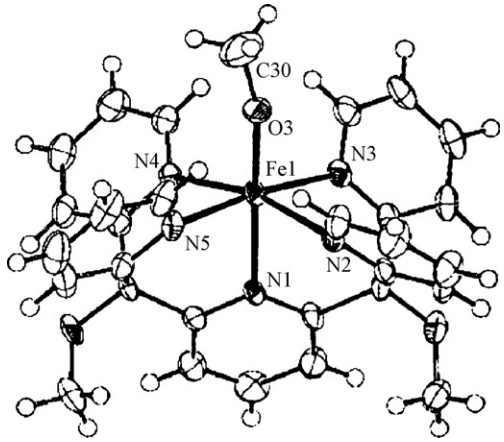

Fig. 22. The crystal structure of $[Fe^{III}(\mathbf{PY}_5)(OMe)]^{2+}$.
(Figure was reproduced from Ref. [136], with permission of the copyright holders.)

to stabilize the resting iron(II) ion relative to the active iron(III) ion in the lipoxygenases, thereby raising the redox potential (and the pK_a value of the coordinated water) in the iron(II) form to facilitate hydrogen abstraction [133].

Prior to 1998, all of the characterized mammalian and plant lipoxygenases utilized iron as the active metal ion for hydrogen abstraction. In 1998, Oliw and coworkers purified and characterized an enzyme from fungus *Gäumannomyces graminis* which can catalyze the peroxidation of linoleic and linolneic acids, two substrates for plant iron lipoxygenases (Fe–LOs). This enzyme, however, contained a manganese ion rather than an iron ion and consequently was classified as the first manganese lipoxygenase (Mn–LO) [134]. Further studies revealed that this Mn–LO can abstract hydrogen in a regio- and stereospecific style just like the Fe–LOs [135]. A mechanism similar to that of the Fe–LOs (in which a M^{III}–OH species is credited for hydrogen abstraction) was proposed.

Although the xanthine oxidases demonstrate a base-assisted hydroxylation of hypoxanthine by the Mo^{VI}–OH functional group, it is not a typical hydrogen atom abstraction process by the Mo^{VI}–OH group (see Fig. 16). In the lipoxygenases, the key active species for hydrogen atom abstraction from the substrate are transition metal hydroxide moieties including Fe^{III}–OH and Mn^{III}–OH. These reactive M^{III}–OH species are rarely involved in enzymatic and chemical oxidation processes. Recently, Stack and coworkers synthesized several inorganic models of the iron and manganese lipoxygenases (Figs. 22 and 23) [136,137]. Both the iron(III) and manganese(III) models, $[Fe^{III}(\mathbf{PY}_5)(OMe)]^{2+}$ and $[Mn^{III}(\mathbf{PY}_5)(OH)]^{2+}$, have demonstrated their capability in hydrogen abstraction from the activated C–H bonds. Particularly, the manganese(III) model contains a manganese(III) hydroxo group, Mn^{III}–OH, and thus resembles the Mn–LO. Using the method introduced by Bordwell and Mayer [138,139], the calculated hydrogen abstraction abilities of the Fe^{III}–OMe and Mn^{III}–OH groups in the models (Figs. 22 and 23) are limited to 83.5 and 82 kcal/mol, respectively, implying that they, like the lipoxygenases, are only capable of abstracting hydrogen from activated C–H bonds.

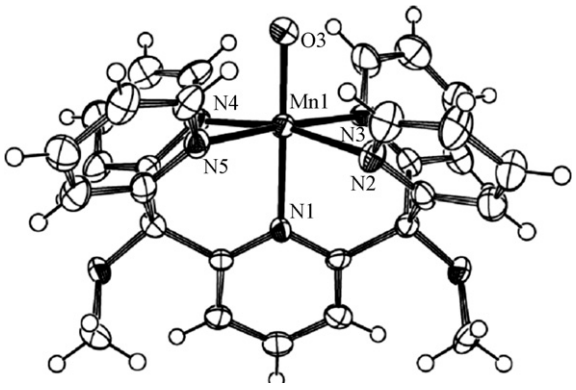

Fig. 23. The crystal structure of $[Mn^{III}(\mathbf{PY}_5)(OH)]^{2+}$.
(Figure was reproduced from Ref. [137], with permission of the copyright holders.)

6. Similarities and differences in reactivity between metal oxo and hydroxo moieties in synthetic models of oxidative enzymes

The preceding sections illustrate that both redox transition metal oxo and hydroxo forms have demonstrated their activity in hydrogen abstraction and/or oxygen transfer processes. The high oxidation state transition metal oxo species are highly powerful oxidants that effect a wide variety of oxidation reactions. Their oxidizing strength and substrate scope are highly metal dependent and coordination environment dependent in both the metalloenzymes and their models. The oxidation processes brought about by high oxidation state transition metal oxo species include abstraction of hydrogen even from robust substrates such as cyclohexane; epoxidation of olefins; dealkylation; and a wide variety of metabolic oxidation processes. While oxidation processes mediated by metal oxo species have been widely studied, the number of known metal hydroxo group mediated oxidation processes is still very small. It is clear that the active iron(III) hydroxo groups of the lipoxygenases are capable of abstracting hydrogen atoms from activated C–H bonds in unsaturated fatty acids, and that the molybdenum(VI) hydroxo group of xanthine oxidases can transfer oxygen to hypoxanthine via a concerted mechanism that also transfers a hydride from the substrate to the Mo^{IV}=S group. For the iron(IV) forms of compound II in the heme enzymes, the situation is complicated. Green clearly demonstrates that the compound II in chloroperoxidases is in an iron(IV) hydroxo form, whereas the forms of compound II (iron(IV) oxo or hydroxo) in HRP, Mb, CCP, and CAT remain under debate.

The key issue is discerning the reactivity similarities and differences between the transition metal oxo and hydroxo forms of a metal while keeping the oxidation state and coordination environment constant. Clarifying the similarities and differences between the two species may explain their respective roles in biological events and ultimately lead to the rational design of selective oxidation catalysts that achieve the desired transformations. Having identical coordination environments and oxidation states, the only viewable difference between the metal oxo and its corresponding metal hydroxo form is the protonation state. Apparently, the protonation states of redox-active metal oxo groups in metalloenzymes are controlled by the protein environment which modulates the redox potential, acid–base properties such as pK_a value, and the reactivity of the active functional group. As described earlier, the dithiolene group of molybdopterin in the molybdenum enzymes and the coordinative flexibility of the iron center in the lipoxygenases have been suspected to play significant roles in modulating the physical chemical properties of the reaction center to facilitate specific reactions. Using the method introduced by Bordwell and Mayer [138,139], the calculated hydrogen abstraction ability of a metal oxo or hydroxo group is directly related to its redox potential and the pK_a value, both of which are modulated by the coordination environment.

Although both iron(IV) oxo and hydroxo groups may exist and match the different reactivity requirements in peroxidases, the protonation states of the active intermediates in most peroxidases remain in question, which stands in the way of confidently

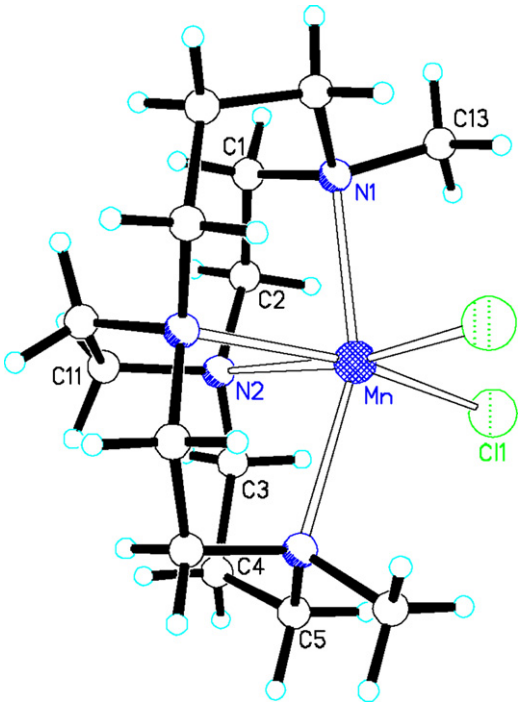

Fig. 24. The X-ray structure of $Mn^{II}(Me_2EBC)Cl_2$.
(Figure was reproduced from Ref. [148], with permission of the copyright holders.)

attributing particular chemical transformations to the iron(IV) oxo or iron(IV) hydroxo intermediate. An alternative approach is using synthetic models as a platform to comprehensively address the similarities and differences between iron(IV) oxo and iron(IV) hydroxo intermediates and then apply the lessons learned from these studies to better understand the active forms of the natural enzymes. A large number of high valent transition metal complexes with an oxo group have been synthesized, characterized and applied in oxidation processes while fewer high valent transition metal complexes with a hydroxo group have been tested for their ability to abstract hydrogen from activated C–H bonds [137,138,140]. Direct comparison of these two types of models is still very rare. The greatest challenge in this work is the tendency for monomeric, high oxidation state, transition metal complexes bearing the hydroxo group to form μ-oxo bridged dimers and/or higher oligomers [141]. Up to now, the only available model for directly comparing the reactivity similarities and differences of a metal oxo group with its corresponding hydroxo group is a manganese(IV) system developed by Busch.

In recent years, Busch and coworkers developed a series of transition metal complexes using one type of ultra rigid, cross-bridged macrocyclic ligand [142–147]. These metal complexes are unusually stable. For example, the half-life of the manganese(II) complex, $Mn(Me_2EBC)Cl_2$ (Fig. 24) (Me_2EBC:4,11-dimethyl-1,4,8,11-tetraazabicyclo[6.6.2]hexadecane), is 13.8 h in 1 M DCl, which is 10^9 times longer than that of the corresponding manganese complex with a porphyrin ligand ($t_{1/2} = 7.4 \times 10^{-6}$ s) [142]. The first monomeric manganese(IV) complex with two hydroxide ligands was successfully synthesized and well characterized by X-ray diffraction, EPR, Raman spectroscopy, UV–visible spectroscopy, cyclic voltammetry, and other techniques (Fig. 25). The presence of methyl groups on the two non-bridging amines prohibits the formation of μ-oxo bridged dimers or oligomers [148]. The manganese(IV) complex is a gentle oxidant with a redox potential of +0.756 V (Mn^{IV}/Mn^{III} vs SHE) and is relatively stable in aqueous solution. In neutral to acidic solution, the manganese(IV) complex is stable for days; while, in base, it gradually

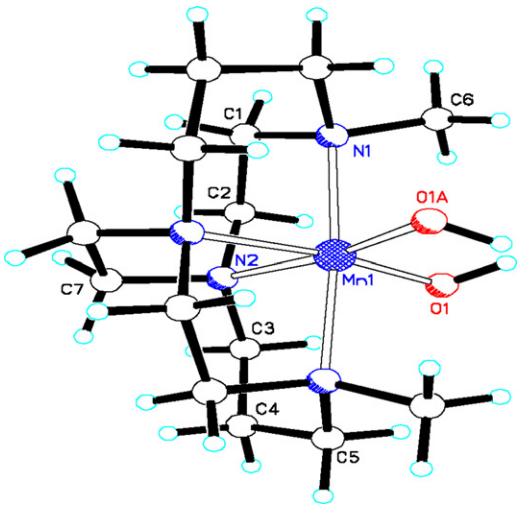

Fig. 25. The X-ray structure of $[Mn^{IV}(Me_2EBC)(OH)_2]^{2+}$.
(Figure was modified from Ref. [150], with permission of the copyright holders.)

degrades to the corresponding manganese(III) complex with an 88% yield. A pH titration of the manganese(IV) complex in aqueous solution gave one accurate pK_a value (6.86) and a second, more approximate pK_a value of 10. The pK_a of 6.86 corresponds to deprotonation of $[Mn(Me_2EBC)(OH)_2]^{2+}$ to form $[Mn(Me_2EBC)(O)(OH)]^{+}$; the approximate pK_a of 10 is related to loss of a second proton to generate $Mn(Me_2EBC)(O)_2$. Apparently, the protonated form of the manganese(IV) complex, that is $[Mn(Me_2EBC)(OH)_2]^{2+}$ is more stable than the corresponding deprotonated forms including $[Mn(Me_2EBC)(O)(OH)]^{+}$ and $Mn(Me_2EBC)(O)_2$, suggesting that the Mn^{IV}=O group could be more active than the corresponding protonated Mn^{IV}–OH group. Because of its two well-separated pK_a values (6.86 and 10), and its relative stability in the aqueous solution, this manganese(IV) complex provides an excellent platform with which to address the reactivity similarities and differences of the transition metal oxo and hydroxo forms while the coordination environment and oxidation state of the metal are conserved (Fig. 26).

The method introduced by Bordwell and Mayer in which the redox potential and the pK_a value of the high valent metal functional group were applied to evaluate its hydrogen atom abstraction ability [138,139], revealed that the hydrogen abstraction abilities of the Mn^{IV}=O group in $[Mn(Me_2EBC)(O)(OH)]^{+}$ and the Mn^{IV}–OH group in $[Mn(Me_2EBC)(OH)_2]^{2+}$ are surprisingly similar (84.3 kcal/mol vs 83.0 kcal/mol) (Fig. 27), and independent experimental tests confirmed their similarities in hydrogen abstraction ability (The hydrogen atom abstraction ability of a high valent metal functional group is thermodynamically equal to the BDE value of the generated O–H bond in the reduced metal

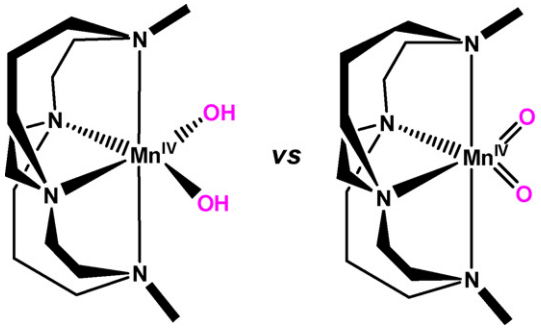

Fig. 26. The manganese(IV) oxo and hydroxo in Busch's manganese(IV) model.

complex.) [149]. Protonation of the Mn^{IV}=O group increases the positive charge on the active center. The overall charge is +2 for $[Mn(Me_2EBC)(OH)_2]^{2+}$ but +1 for $[Mn(Me_2EBC)(O)(OH)]^{+}$. Protonation was expected to change both the electronic properties and reactivity of the metal center, but the calculated hydrogen abstraction abilities of the Mn^{IV}–OH group in $[Mn(Me_2EBC)(OH)_2]^{2+}$ and the Mn^{IV}=O group in $[Mn(Me_2EBC)(O)(OH)]^{+}$ are very similar. The change of the electronic properties and reactivity by protonation of the Mn^{IV}=O has apparently been largely compensated by the increase of the charge in the reaction center. In the calculation, this is reflected by the two similar pK_a values, 5.87 and 6.86, respectively. If the charge of the reaction center having the Mn^{IV}=O and Mn^{IV}–OH groups were identical, that is $[Mn^{IV}{=}O]^{n+}$ vs $[Mn^{IV}{-}OH]^{n+}$, one may expect that their oxidizing power for hydrogen abstraction would be significantly different. These results strongly suggest that protonation of a metal oxo group may not change its oxidizing power seriously, at least from the thermodynamic perspective.

Although thermodynamically, the Mn^{IV}–OH group in $[Mn(Me_2EBC)(OH)_2]^{2+}$ and the Mn^{IV}=O group in $[Mn(Me_2EBC)(O)(OH)]^{+}$ demonstrate similar hydrogen abstraction ability; the $[Mn(Me_2EBC)(O)(OH)]^{+}$ species dominant at pH 8.4 gives a rate more than 10 times faster than that exhibited by the $[Mn(Me_2EBC)(OH)_2]^{2+}$ species which is predominant at pH 4.0. Since the hydrogen abstraction ability of $[Mn(Me_2EBC)(O)(OH)]^{+}$ at pH 8.4 may be reflective of both the Mn^{IV}=O and Mn^{IV}–OH groups; the authors further investigated the hydrogen abstraction abilities of the manganese(IV) complex at pH values of 4.0 and 13.4 where $[Mn(Me_2EBC)(OH)_2]^{2+}$ and $Mn(Me_2EBC)(O)_2$ each respectively predominate. These studies provide a clean comparison of the reactivity differences between the metal oxo and hydroxo species (Fig. 26) [150]. In these studies, the Mn^{IV}=O group abstracted hydrogen at rates approximately 40 times faster than the Mn^{IV}–OH group for a series of substrates (Table 1). For example, the k_{oxo}/k_{OH} ratio is about 44 for hydrogen abstraction from 9,10-dihydroanthracene. Kinetic isotope effects demonstrated that hydrogen atom transfer is the rate determining step in both cases. More interestingly, in the case of hydrogen abstraction from 9,10-dihydroanthracene, the calculated activation parameters from the temperature range of 288–318 K revealed that the activation entropy contributes a 10.6-fold rate increase while the activation enthalpy contributes an approximately 5.4-fold rate increase. These significant rate differences between the Mn^{IV}=O and the corresponding Mn^{IV}–OH species demonstrate that the protonation state of a transition metal oxo center strongly influences its efficacy

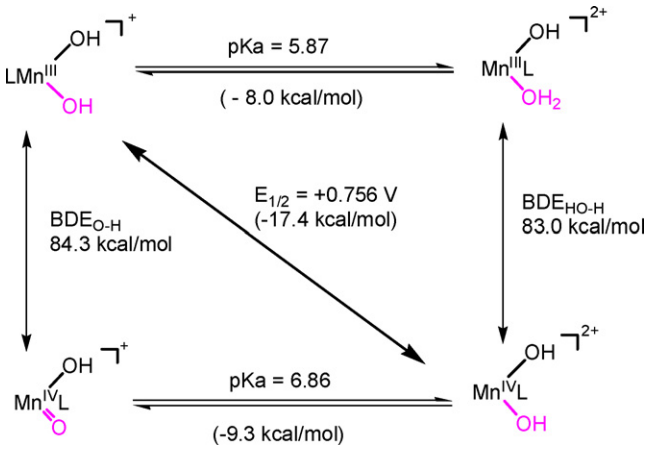

Fig. 27. Theoretical calculations of hydrogen abstraction capability of the Mn^{IV}–OH and Mn^{IV}=O groups in the corresponding $Mn^{IV}(Me_2EBC)$ complexes.
(Figure was reproduced from Ref. [149], with permission of the copyright holders.)

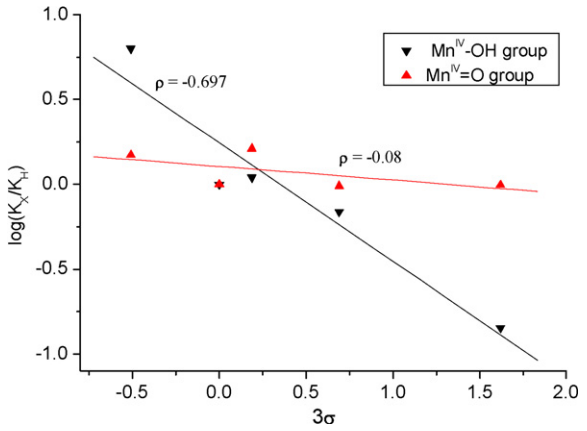

Fig. 28. Hammett plot for the oxygenation of triarylphosphines by Mn^{IV}–OH and Mn^{IV}=O groups in the corresponding $Mn^{IV}(Me_2EBC)$ complexes in acetone/water (4:1) at 293 K.
(Figure was modified from Ref. [151], with permission of the copyright holders.)

for hydrogen abstraction even though the protonation state has little influence on the thermodynamic oxidizing power.

Using Busch's manganese(IV) model, Yin and coworkers continued investigating differences in oxidative reactivity between the Mn^{IV}=O and its corresponding Mn^{IV}–OH functional group through oxidation of triphenylphosphine and its derivatives [151] and found that the Mn^{IV}=O group in $Mn(Me_2EBC)(O)_2$ is capable of oxygenation of triphenylphosphine. When hydroxylated species were investigated, an inverse solvent isotope effect revealed that the Mn^{IV}–OH group in $[Mn(Me_2EBC)(OH)(OH_2)]^{3+}$ rather than the Mn^{IV}–OH group in $[Mn(Me_2EBC)(OH)_2]^{2+}$ served as the oxidant for triphenylphosphine. In other words, further protonation of the $[Mn(Me_2EBC)(OH)_2]^{2+}$ species to form the $[Mn(Me_2EBC)(OH)(OH_2)]^{3+}$ species is essential for oxygenation by the Mn^{IV}–OH group. Surprisingly, and in contrast to observations for the hydrogen abstraction reactions, the oxygenation rate by the Mn^{IV}=O group in $Mn(Me_2EBC)(O)_2$ is comparable with that of the Mn^{IV}–OH group in $[Mn(Me_2EBC)(OH)(OH_2)]^{3+}$. However, a Hammett plot of substituent effects for the triarylphosphine substrates revealed that oxygenations by the Mn^{IV}=O and Mn^{IV}–OH groups proceed by difference mechanisms (Fig. 28). The ρ slope of −0.697 for the Mn^{IV}–OH species supports the development of positive charge in the transition state suggesting an electron transfer mechanism; whereas the ρ slope of −0.08 for oxygenation by the Mn^{IV}=O group suggests a concerted oxygen transfer mechanism in which no obvious charge development occurs in the transition state. The high charge of the $[Mn(Me_2EBC)(OH)(OH_2)]^{3+}$ species may also facilitate electron transfer from triphenylphosphine to the Mn^{IV}–OH group. From the hydrogen abstraction and oxygenation studies involving Busch's manganese(IV) model, the protonation state of the Mn^{IV}=O group definitely affects the intrinsic reactivity of the manganese(IV) center, even though the thermodynamically oxidizing power may not be changed significantly. These reactivity differences are reflected in different reaction rates for hydrogen abstraction and variable mechanistic pathways for oxygenation.

In addition to the work involving Busch's manganese(IV) model, Fuji and coworkers investigated the structure–reactivity relationship for three transient intermediates of the Mn(Salen) catalyst including O=Mn^{IV}(salen), HO–Mn^{IV}(salen), and H_2O–Mn^{III}($salen^{+\bullet}$) (Fig. 29) [152]. Based on various spectroscopic techniques, the three intermediates differ only in their degree of protonation. Other techniques, however, showed that their structural and electronic features are strikingly different: The Mn–O bond length of HO–Mn^{IV}(salen) (1.83 Å) is considerably longer than that of O=Mn^{IV}(salen) (1.58 Å); the electronic configuration of

Table 1
The second order rate constants for hydrogen abstraction from substrates with $[Mn^{IV}(Me_2EBC)(OH)_2]^{2+}$ and $Mn^{IV}(Me_2EBC)(O)_2$ at pH 4.0 and pH 13.4 (Table was reproduced from Ref. [151], with permission of the copyright holders).

Substrate	BDE_{CH} (kcal/mol)	k_{2OH} at pH 4.0 ($M^{-1}\,s^{-1}$)	k_{2OXO} at pH 13.4 ($M^{-1}\,s^{-1}$)	k_{2OXO}/k_{2OH}
Xanthene	75.5	0.00107	0.048	44
1,4-Cyclohexadiene	76	3.64×10^{-4}	0.0159	44
9,10-Dihydroxyanthracene	78	3.52×10^{-4}	0.01496	43
Fluorene	80	$\sim 2.5 \times 10^{-4}$	0.00912	36

Reaction conditions: The reactions were carried out in 4:1 acetone/water at 288 K. The initial concentration of substrate was 40 mM and the initial concentration of manganese(IV) complex was 4 mM.

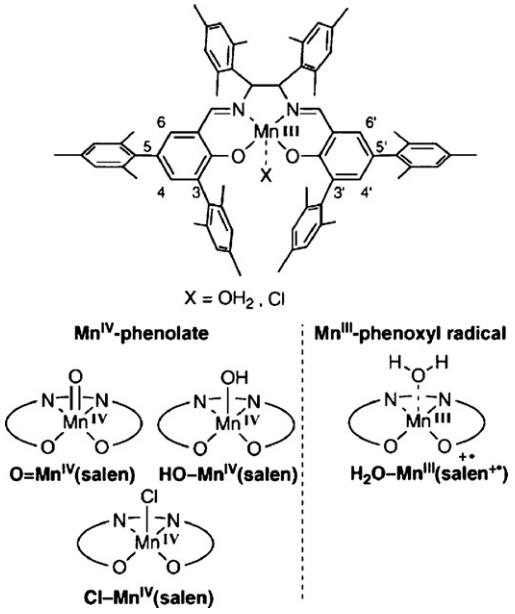

Fig. 29. Four transient intermediates from the asymmetric epoxidation catalyst Mn(salen).
(Figure was modified from Ref. [152], with permission of the copyright holders.)

H_2O–Mn^{III}(salen$^{+\bullet}$) is Mn^{III}–phenoxyl radical, while those of O=Mn^{IV}(salen) and HO–Mn^{IV}(salen) are Mn^{IV}–phenolate. Unfortunately, only the O=Mn^{IV}(salen) can transfer oxygen to phosphine and sulfide substrates as well as abstract hydrogen from weak C–H bonds. Consequently, attempts to directly compare reactivity differences between the different manganese salen intermediates were not successful.

Unlike peroxidases in which both iron(IV) oxo and hydroxo functional groups may occur as the key active intermediates, only iron(III) and manganese(III) hydroxo groups have been proposed to mediate hydrogen abstraction in the lipoxygenase; the deprotonated iron(III) and manganese(III) oxo forms have never been reported. As described earlier, Stack and coworkers synthesized a $[Mn^{III}(\mathbf{PY}_5)(OH)]^{2+}$ complex which has a Mn^{III}–OH functional group as a model for manganese lipoxygenase (Fig. 23) [137]. The calculated hydrogen abstraction ability of the Mn^{III}–OH group in $[Mn^{III}(\mathbf{PY}_5)(OH)]^{2+}$ is limited to 82 kcal/mol. Hydrogen abstraction experiments also confirmed its capability, and hydrogen atom transfer was proposed as the rate determining step, just as it is in the catalytic cycle of the lipoxygenases. However, there were no available reactivity data for the corresponding Mn^{III}=O group in Stack's model. Borovik and coworkers recently developed a tris[(N′-tert-butylureaylato)-N-ethyl)]aminato ligand (H_6buea). Using the H_6buea ligand, they developed a series of monomeric iron and manganese complexes including iron(II) and manganese(II) hydroxo, iron(III) and manganese(III) hydroxo and oxo, and manganese(IV) oxo complexes (Figs. 30 and 31) [153–155]. The calculated hydro-

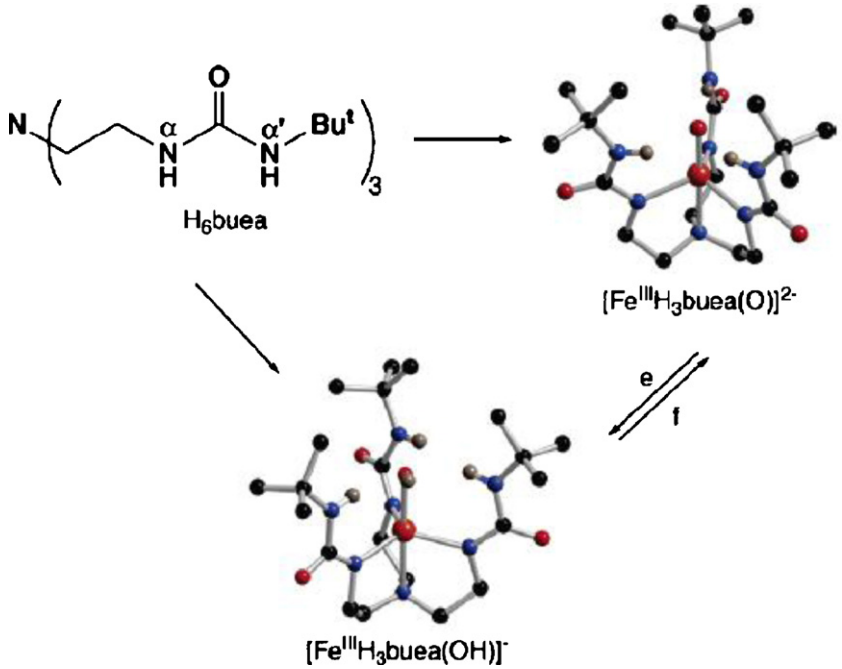

Fig. 30. X-ray structure of $[Fe^{III}(H_3buea)(OH)]^-$ and $[Fe^{III}(H_3buea)(O)]^{2-}$.
(Figure was modified from Ref. [154], with permission of the copyright holders.)

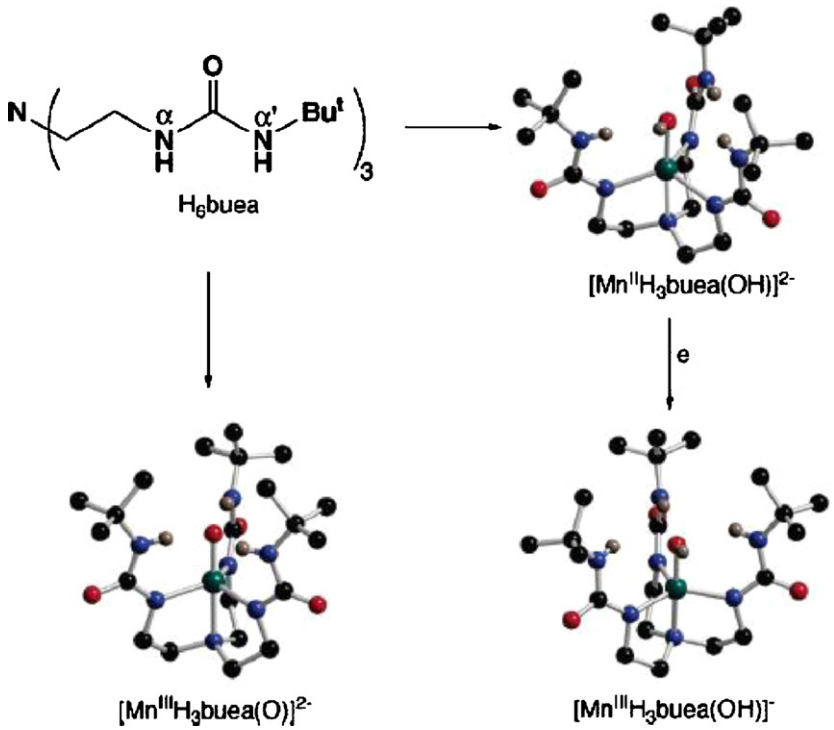

Fig. 31. X-ray stucture of $[Mn^{II}(H_3buea)(O)]^{2-}$, $[Mn^{III}(H_3buea)(OH)]^{-}$ and $[Mn^{III}(H_3buea)(O)]^{2-}$. (Figure was modified from Ref. [154], with permission of the copyright holders.)

gen abstraction abilities of the Fe^{III}=O group in $[Fe^{III}(H_3buea)(O)]^{2-}$ and the Mn^{III}=O group in $[Mn^{III}(H_3buea)(O)]^{2-}$ are limited to 66 and 77 kcal/mol, respectively. Both the Fe^{III}=O and Mn^{III}=O groups are capable of hydrogen abstraction from the activated C–H bond in substrates such as 9,10-dihydroanthracene, but the corresponding Fe^{III}–OH group in $[Fe^{III}(H_3buea)(OH)]^{-}$ and the Mn^{III}–OH group in $[Mn^{III}(H_3buea)(OH)]^{-}$ are incapable of abstracting hydrogen from the tested substrates including 9,10-dihydroanthracene, 1,4-cyclohexadiene, triphenylmethane, diphenylmethane and 2,3-dimethyl-2-butene. Thus, direct comparisons between metal oxo and metal hydroxo species are not available for Borovik's model. Very interestingly, because of the extra low redox potential of the $Mn^{III/IV}$(O) couple (−1.0 V) and the large pK_a value of 28.3 for $[Mn^{III}(H_3buea)(OH)]^{-}$, the authors proposed that hydrogen abstraction by the Mn^{III}=O group in $[Mn^{III}(H_3buea)(O)]^{2-}$ proceeds by separate proton and electron transfer steps, where proton transfer occurs prior to electron transfer. Although they have different coordination environments, the reactivity differences between the Mn^{III}=O group in Borovik's $[Mn^{III}(H_3buea)(O)]^{2-}$ model and the protonated Mn^{III}–OH group in Stack's $[Mn^{III}(\mathbf{PY}_5)(OH)]^{2+}$ model may provide clues for understanding why the lipoxygenases employ the Fe^{III}–OH or Mn^{III}–OH group rather than the corresponding Fe^{III}=O or Mn^{III}=O group for hydrogen abstraction from the unsaturated fatty acid.

7. Conclusion

Recent studies have revealed that the form of the active functional groups to facilitate oxidation processes in versatile metalloenzymes could be enzyme dependent. While the iron(IV) oxo form of compound I has been well accepted in all of the heme enzymes, the available evidence supports that the compound II in CPO is in the iron(IV) hydroxo form. The iron(IV) oxo form of compound II in most peroxidases is still debatable. Among the molybdenum enzymes, xanthine oxidase employs a Mo^{VI}–OH group for hydroxylation, whereas a Mo^{VI}=O group plays the key role in other molybdenum enzymes. In the lipoxygenases, evidence supports iron(III) or manganese(III) hydroxo species, rather than their oxo forms, as key intermediates in hydrogen abstraction from unsaturated fatty acids. Clarifying the structure and reactivity similarities and differences between the metal oxo intermediates and their corresponding metal hydroxo forms would obviously promote better understanding the roles they may play in oxidation processes.

Although there are not enough data on biological oxidation processes to fully explore the roles of metal oxo and metal hydroxo intermediates in enzymes, the information from existing studies has suggested simple, appropriate synthetic models. Among the different models, Busch's manganese(IV) complex provides the most information about the reactivity similarities and differences between a transition metal oxo and its corresponding metal hydroxo form. In Busch's model, protonation of the Mn^{IV}=O group does not change its oxidizing power significantly for hydrogen atom abstraction, that is, 83 kcal/mol in Mn^{IV}–OH form vs 84.3 kcal/mol in Mn^{IV}=O form. Protonation does, however, change the reactivity significantly. Although the hydrogen abstraction mechanisms mediated by the Mn^{IV}=O and Mn^{IV}–OH forms are similar, protonation of the Mn^{IV}=O group significantly decreases its efficacy. For the oxidation of triphenylphosphine, the mechanism of Mn^{IV}=O mediated oxidation is significantly different from that of Mn^{IV}–OH mediated oxidation. The Mn^{IV}=O group in $Mn(Me_2EBC)(O)_2$ can transfer oxygen to the substrate by way of a concerted oxygen transfer mechanism, whereas one of the Mn^{IV}–OH groups in $[Mn(Me_2EBC)(OH)_2]^{2+}$ needs to be further protonated to generate $[Mn(Me_2EBC)(OH)(OH_2)]^{3+}$, and then the last Mn^{IV}–OH group in $[Mn(Me_2EBC)(OH)(OH_2)]^{3+}$ serves to oxygenate the triphenylphosphine through an electron transfer process, not via a concerted oxygen transfer process. The similarities and differences for the reactivities of the Mn^{IV}=O and Mn^{IV}–OH forms in Busch's model have provided significant clues for understanding the similar properties of active intermediates in metalloenzymes. One can observe

that in the models developed by Busch, Borovik and Stack, the protonation state of a redox metal oxo group may not affect its thermodynamic oxidizing power significantly; but the reactivity profiles and reaction rates may none-the-less change appreciably. Similarly, in the peroxidases, the protonated and un-protonated iron(IV) forms of compound II could have similar oxidizing power, but they may demonstrate different reactivities to match the oxidation requirements in specific peroxidases. However, the current data concerning a variety of metalloenzymes are apparently not enough to provide a comprehensive understanding of their mechanisms. Further studies are still essential to elucidate the similarities and differences between the metal oxo and corresponding metal hydroxo forms of synthetic, biomimetic, oxidation catalysts. Knowledge of these synthetic models will promote understanding of the enzymatic mechanisms and the design of selective oxidation catalysts for the targeted substrates.

Acknowledgement

This work was supported by National Natural Science Foundation of China (No. 20973069).

References

[1] B. Meunier (Ed.), Biomimetic Oxidations Catalyzed by Transition Metal Complexes, Imperial College Press, Singapore, 2000.
[2] J.S. Valentine, C.S. Foote, A. Greenberg, J.F. Liebman (Eds.), Active Oxygen In Biochemistry, Black Academic & Professional, London, 1995.
[3] E.M. McGarrigle, D.G. Gilheany, Chem. Rev. 105 (2005) 1563.
[4] J.T. Groves, J. Chem. Educ. 62 (1985) 928.
[5] S.T. Prigge, J.C. Boyington, M. Faig, K.S. Doctor, B.J. Gaffney, L.M. Amzel, Biochimie 79 (1997) 629.
[6] S. Fukuzumi, Helv. Chim. Acta 89 (2006) 2425.
[7] R. Hille, Chem. Rev. 96 (1996) 2757.
[8] R.K Behan, M.T. Green, J. Inorg. Biochem. 100 (2006) 448.
[9] M. Sono, M.P. Roach, E.D. Coulter, J.H. Dawson, Chem. Rev. 96 (1996) 2841.
[10] P.R. Ortiz de Montellano (Ed.), Cytochrome P450: Structure, Mechanism And Biochemistry, Plenum Press, New York, 1986.
[11] I.G. Denisov, T.M. Makris, S.G. Sligar, I. Schlichting, Chem. Rev. 105 (2005) 2253.
[12] W. Woggon, Acc. Chem. Res. 38 (2005) 127.
[13] P. Jones, H.B. Dunford, J. Inorg. Biochem. 99 (2005) 2292.
[14] T.G. Traylor, P.S. Traylor, in: J.S. Valentine, C.S. Foote, A. Greenberg, J.F. Liebman (Eds.), Active Oxygen In Biochemistry, Black Academic & Professional, London, 1995, p. 84.
[15] J.H. Dawson, R.H. Holm, J.R. Trudell, G. Barth, R.E. Linder, E. Bunnenberg, C. Djerassi, S.C. Tang, J. Am. Chem. Soc. 98 (1976) 3707.
[16] M. Sono, L.A. Andersson, J.H. Dawson, J. Biol. Chem. 257 (1982) 8308.
[17] M. Sono, J.H. Dawson, J. Biol. Chem. 257 (1982) 5496.
[18] H.I. Liu, M. Sono, S. Kadkhodayan, L.P. Hager, B. Hedman, K.O. Hodgson, J.H. Dawson, J. Biol. Chem. 270 (1995) 10544.
[19] P.R. Ortiz de Montellano, Annu. Rev. Pharmacol. Toxicol. 32 (1992) 89.
[20] S. Adachi, S. Nagano, K. Ishimori, Y. Watanabe, I. Morishima, T. Egawa, T. Kitagawa, R. Makino, Biochemistry 32 (1993) 241.
[21] I.C. Gunsalus, J.R. Meeks, J.D. Lipscomb, P. Debrunner, E. Munk, in: O. Hyaaishi (Ed.), Molecular Mechanisms of Oxygen Activation, Academic Press, New York, 1974, p. 559.
[22] D.L. William-Smith, P.J. Morrison, Biochim. Biophys. Acta 405 (1975) 253.
[23] D.L. William-Smith, K. Patel, Biochim. Biophys. Acta 405 (1975) 243.
[24] H. Yamada, R. Makino, I. Yamazaki, Arch. Biochem. Biophys. 169 (1975) 344.
[25] J.T. Groves, Proc. Natl. Acad. Sci. U.S.A. 100 (2003) 3569.
[26] Y. Zhu, R.B. Silverman, Biochemistry 47 (2008) 2231.
[27] H. Hersleth, U. Ryde, P. Rydberg, C.H. Görbitz, K.K. Andersson, J. Inorg. Biochem. 100 (2006) 460.
[28] D.G. Kellner, S. Hung, K.E. Weiss, S.G. Sligar, J. Biol. Chem. 277 (2002) 9641.
[29] M.J. Benecky, J.E. Frew, N. Scowen, P. Jones, B.M. Hoffman, Biochemistry 32 (1993) 11929.
[30] T. Egawa, H. Shimada, Y. Ishimura, Biochem. Biophys. Res. Commun. 201 (1994) 1464.
[31] L.P. Hager, D.L. Doubek, R.M. Silverstein, J.H. Hargis, J.C. Martin, J. Am. Chem. Soc. 94 (1972) 4364.
[32] D.M. Davies, P. Jones, D. Mantle, Biochem. J. 157 (1976) 247.
[33] P. Jones, D.N. Middlemiss, Biochem. J. 130 (1972) 411.
[34] T.D. Pfister, A.J. Gengenbach, S. Syn, Y. Lu, Biochemistry 40 (2001) 14942.
[35] R. Raag, B.A. Swanson, T.L. Poulos, P.R. Ortiz de Montellano, Biochemistry 29 (1990) 8119.
[36] B.A. Swanson, D.R. Dutton, J.M. Lunetta, C.S. Yang, P.R. Ortiz de Montellano, J. Biol. Chem. 266 (1991) 19258.
[37] P.R. Ortiz de Montellano, Acc. Chem. Res. 20 (1987) 289.
[38] G.D. DePillis, H. Wariishi, M.H. Gold, P.R. Ortiz de Montellano, Arch. Biochem. Biophys. 280 (1990) 217.
[39] R.Z. Harris, H. Wariishi, M.H. Gold, P.R. Ortiz de Montellano, J. Biol. Chem. 266 (1991) 8751.
[40] G.D. DePillis, P.R. Ortiz de Montellano, Biochemistry 28 (1989) 7947.
[41] Z.S. Farhangrazi, B.R. Copeland, T. Nakayama, T. Amachi, I. Yamazaki, L.S. Powers, Biochemistry 33 (1994) 5647.
[42] Z.S. Farhangrazi, R. Sinclair, L. Powers, I. Yamazaki, Biochemistry 34 (1995) 14970.
[43] B. He, R. Sinclair, B.R. Copeland, R. Makino, L.S. Powers, I. Yamazaki, Biochemistry 35 (1996) 2413.
[44] D. Dolphin, A. Forman, D.C. Borg, J. Fajer, R.H. Felton, Proc. Natl. Acad. Sci. U.S.A. 68 (1971) 614.
[45] R.A. Leising, B.A. Brennan, L. Que Jr., B.G. Fox, E. Munck, J. Am. Chem. Soc. 113 (1991) 3988.
[46] W.A. Oertling, R.T. Kean, R. Wever, G.T. Babcock, Inorg. Chem. 29 (1990) 2633.
[47] J.E. Penner-Hahn, E.S. Kim, T.J. McMurry, M. Renner, A.L. Balch, J.T. Groves, J.H. Dawson, K.O. Hodgson, J. Am. Chem. Soc. 108 (1986) 7819.
[48] T. Hamada, T. Fukuda, H. Imanishi, T. Katsuki, Tetrahedron 52 (1996) 515.
[49] D.E. Lansky, B. Mandimutsira, B. Ramdhanie, M. Clausén, J. Penner-Hahn, S.A. Zvyagin, J. Telser, J. Krzystek, R.Q. Zhan, Z.P. Ou, K.M. Kadish, L. Zakharov, A.L. Rheingold, D.P. Goldberg, Inorg. Chem. 44 (2005) 4485.
[50] B.S. Mandimutsira, B. Ramdhanie, R.C. Todd, H.L. Wang, A.A. Zareba, R.S. Czernuszewicz, D.P. Goldberg, J. Am. Chem. Soc. 124 (2002) 15170.
[51] Y. Shiro, M. Takeda, I. Morishima, J. Am. Chem. Sci. 110 (1988) 4030.
[52] J.E. Penner-Hahn, M. Benfatto, B. Hedman, T. Takahashi, S. Doniach, J.T. Groves, K.O. Hodgson, Inorg. Chem. 25 (1986) 2255.
[53] A.L. Balch, G.N. La Mar, L. Latos-Grazynski, M.W. Renner, V. Thanabal, J. Am. Chem. Soc. 107 (1985) 3003.
[54] K. Qin, C.D. Incarvito, A.L. Rheingold, K.H. Theopold, J. Am. Chem. Soc. 124 (2002) 14008.
[55] C.G. Miller, S.W. Gordon-Wylie, C.P. Horwitz, S.A. Strazisar, D.K. Peraino, G.R. Clark, S.T. Weintraub, T.J. Collins, J. Am. Chem. Soc. 120 (1998) 11540.
[56] A. Dovletoglou, T.J. Meyer, J. Am. Chem. Soc. 116 (1994) 215.
[57] D. Chin, A.L. Balch, G.N. La Mar, J. Am. Chem. Soc. 102 (1980) 1446.
[58] J.T. Groves, Z. Gross, M.K. Stern, Inorg. Chem. 33 (1994) 5065.
[59] J.P. Collman, L. Zeng, J.I. Brauman, Inorg. Chem. 43 (2004) 2672.
[60] M. Newcomb, D. Aebisher, R. Shen, R.E.P. Chandrasena, P.F. Hollenberg, M.J. Coon, J. Am. Chem. Soc. 125 (2003) 6064.
[61] F.T. de Oliveira, A. Chanda, D. Banerjee, X. Shan, S. Mondal, L. Que Jr., E.L. Bominaar, E. Münck, T.J. Collins1, Science 315 (2007) 835.
[62] J.T. Groves, T.E. Nemo, R.S. Myers, J. Am. Chem. Soc. 101 (1979) 1032.
[63] N.R. Orme-Johnson, D.R. Light, R.W. White-Stevens, W.H. Orme-Johnson, J. Biol. Chem. 254 (1979) 2103.
[64] S. Nakajin, M. Shinoda, M. Haniu, J.E. Shively, P.F. Hall, J. Biol. Chem. 259 (1984) 3971.
[65] J.T. Groves, P. Viski, J. Am. Chem. Soc. 111 (1989) 8537.
[66] J. Bernadou, A. Fabiano, B. Meunier, J. Am. Chem. Soc. 116 (1994) 9375.
[67] J.T. Groves, J. Lee, S.S. Marla, J. Am. Chem. Soc. 119 (1997) 6269.
[68] J.H. Espenson, Coord. Chem. Rev. 249 (2005) 329.
[69] Y. Moro-oka, M. Akita, Catal. Today 41 (1998) 327.
[70] C. Che, Pure Appl. Chem. 67 (1995) 225.
[71] D. Mansuy, Coord. Chem. Rev. 125 (1993) 129.
[72] W.D. Kerber, D.P. Goldberg, J. Inorg. Biochem. 100 (2006) 838.
[73] M.T. Green, J.H. Dawson, H.B. Gray, Science 304 (2004) 1653.
[74] R.K. Behan, L.M. Hoffart, K.L. Stone, C. Krebs, M.T. Green, J. Am. Chem. Soc. 128 (2006) 11471.
[75] K.L. Stone, R.K. Behan, M.T. Green, Proc. Natl. Acad. Sci. U.S.A. 102 (2005) 16563.
[76] M.T. Green, J. Am. Chem. Soc. 128 (2006) 1902.
[77] K.L. Stone, R.K. Behan, M.T. Green, Proc. Natl. Acad. Sci. U.S.A. 103 (2006) 12307.
[78] G.I. Berglund, G.H. Carlsson, A.T. Smith, H. Szöke, A. Henriksen, J. Hajdu, Nature 417 (2002) 463.
[79] J.E. Penner-Hahn, T.M.J. cMurry, M. Renner, L. Latos-Grazynsky, K.S. Eble, I.M. Davis, A.L. BalchII, J.T. Groves, J.H. Dawson, K. Hodgson, J. Biol. Chem. 258 (1983) 12761.
[80] A.J. Sitter, C.M. Reczek, J. Terner, J. Biol. Chem. 260 (1985) 7515.
[81] R.K. Behan, M.T. Green, J. Inorg. Biochem. 100 (2006) 448.
[82] R. Davydov, R.L. Osborne, S.H. Kim, J.H. Dawson, B.M. Hoffman, Biochemistry 47 (2008) 5147.
[83] C. Kisker, H. Schindelin, A. Pacheco, W.A. Wehbi, R.M. Garrett, K.V. Rajagopalan, J.H. Enemark, D.C. Rees, Cell 91 (1997) 973.
[84] B.E. Schultz, R. Hille, R.H. Holm, J. Am. Chem. Soc. 117 (1999) 827.
[85] M.S. Brody, R. Hille, Biochim. Biophys. Acta 1253 (1995) 133.
[86] A.V. Astashkin, M.L. Mader, A. Pacheco, J.H. Enemark, A.M. Raitsimring, J. Am. Chem. Soc. 122 (2000) 5294.
[87] H.L. Wilson, K.V. Rajagopalan, J. Biol. Chem. 279 (2004) 15105.
[88] G.N. George, R.M. Garrett, R.C. Prince, K.V. Rajagopalan, Inorg. Chem. 43 (2004) 8456.
[89] A. Pacheco, J.T. Hazzard, G. Tollin, J.H. Enemark, J. Biol. Inorg. Chem. 4 (1999) 390.
[90] S. Gardlik, K.V. Rajagopalan, J. Biol. Chem. 266 (1991) 4889.
[91] R. Hille, V. Massey, J. Biol. Chem. 257 (1982) 8898.
[92] R. Huber, P. Hof, R.O. Duarter, J.J.G. Moura, I. Moura, M.Y. Liu, J. LeGall, R. Hille, M. Archer, M. Romäo, Proc. Natl. Acad. Sci. U.S.A. 93 (1996) 8846.

[93] R. Eisenberg, Prog. Inorg. Chem. 12 (1970) 295.
[94] J.P. Caradonna, P.R. Reddy, R.H. Holm, J. Am. Chem. Soc. 110 (1988) 2139.
[95] S.K. Das, P.K. Chaudhury, D. Biswas, S. Sarkar, J. Am. Chem. Soc. 116 (1994) 9061.
[96] P.K. Chaudhury, S.K. Das, S. Sarkar, Biochem. J. 319 (1996) 953.
[97] C. Lorber, M.R. Plutino, L.I. Elding, E. Nordlander, J. Chem. Soc., Dalton Trans. (1997) 3997.
[98] M.L. Mader, M.D. Carducci, J.H. Enemark, Inorg. Chem. 39 (2000) 525.
[99] R. Hille, H. Sprecher, J. Biol. Chem. 262 (1987) 10914.
[100] G.J.J. Chen, J.W. McDonald, W.E. Newton, Inorg. Chem. 16 (1976) 2612.
[101] J.M. Berg, R.H. Holm, J. Am. Chem. Soc. 107 (1985) 917.
[102] J.M. Berg, R.H. Holm, J. Am. Chem. Soc. 107 (1985) 925.
[103] R.J. Greenwood, G.L. Wilson, J.R. Pilbrow, A.G. Wedd, J. Am. Chem. Soc. 115 (1993) 5385.
[104] B.D. Howes, R.C. Bray, R.L. Richards, N.A. Turner, B. Bennett, D.J. Lowe, Biochemistry 35 (1996) 1432.
[105] M. Xia, R. Dempski, R. Hille, J. Biol. Chem. 274 (1999) 3323.
[106] K. Okamoto, K. Matsumoto, R. Hille, B.T. Eger, E.F. Pai, T. Nishino, Proc. Natl. Acad. Sci. U.S.A. 104 (2004) 7931.
[107] A.L. Stockert, S.S. Shinde, R.F. Anderson, R. Hille, J. Am. Chem. Soc. 124 (2002) 14554.
[108] E. Choi, A.L. Stockert, S. Leimkühler, R. Hille, J. Inorg. Biochem. 98 (2004) 841.
[109] C.J. Doonan, A. Stockert, R. Hille, G.N. George, J. Am. Chem. Soc. 127 (2005) 4518.
[110] P. Ilich, R. Hille, J. Phys. Chem. B 103 (1999) 5406.
[111] C.J. Doonan, N.D. Rubie, K. Peariso, H.H. Harris, S.Z. Knottenbelt, G.N. George, C.G. Young, M.L. Kirk, J. Am. Chem. Soc. 130 (2008) 55.
[112] E.I. Stiefel, K.F. Miller, A.E. Bruce, J.L. Corbin, J.M. Berg, K.O. Hodgson, J. Am. Chem. Soc. 102 (1980) 3624.
[113] I.G. Dance, A.G. Wedd, I.W. Boyd, Aust. J. Biochem. 31 (1978) 519.
[114] A. Thapper, J.P. Donahue, K.B. Musgrave, M.W. Willer, E. Nordlander, B. Hedman, K.O. Hodgson, R.H. Holm, Inorg. Chem. 38 (1999) 4104.
[115] J. Wang, S. Groysman, S.C. Lee, R.H. Holm, J. Am. Chem. Soc. 129 (2007) 7512.
[116] S.T. Prigge, J.C. Boyington, M. Faig, K.S. Doctor, B.J. Gaffney, L.M. Amzel, Biochimie. 79 (1997) 629.
[117] J.C. Boyington, B.J. Gaffney, L.M. Amzel, Science 260 (1993) 1482.
[118] W. Minor, J. Steczko, B. Stec, Z. Otwinowski, J.T. Bolin, R. Walter, B. Axelrod, Biochemistry 35 (1996) 10687.
[119] D.R. Tomchick, P. Phan, M. Cymborowski, W. Minor, T.R. Holman, Biochemistry 40 (2001) 7509.
[120] M.L. Neidig, A.T. Wecksler, G. Schenk, T.R. Holman, E.I. Solomon, J. Am. Chem. Soc. 129 (2007) 7531.
[121] E. Sigal, C.S. Craik, E. Highland, D. Grunberger, L.L. Costello, R.A.F. Dixon, J.A. Nadel, Biochem. Biophys. Res. Commun. 157 (1988) 457.
[122] E. Sigal, Am. J. Physiol. 260 (1991) L13.
[123] M.A. Pavlosky, Y. Zhang, T.E. Westre, Q. Gan, E.G. Pave, C. Campochiaro, B. Hedman, K.O. Hodgson, E.I. Solomon, J. Am. Chem. Soc. 117 (1995) 4317.
[124] M. Hamberg, B. Samuelsson, J. Biol. Chem. 242 (1967) 5329.
[125] G. Coffa, A.N. Imber, B.C. Maguire, G. Laxmikanthan, C. Schneider, B.J. Gaffney, A.R. Brash, J. Biol. Chem. 280 (2005) 38756.
[126] H. Kitaguchi, K. Ohkubo, S. Ogo, S. Fukuzumi, J. Am. Chem. Soc. 127 (2005) 6605.
[127] M.H. Glickman, J. Wiseman, J.P. Klinman, J. Am. Chem. Soc. 116 (1994) 793.
[128] C.C. Hwang, C.B. Grissom, J. Am. Chem. Soc. 116 (1994) 795.
[129] A. Thibblin, J. Phys. Org. Chem. 1 (1988) 161.
[130] A. Thibblin, P. Ahlberg, Chem. Soc. Rev. 18 (1989) 209.
[131] M.H. Glickman, J.P. Klinman, Biochemistry 34 (1995) 14077.
[132] K.W. Rickert, J.P. Klinman, Biochemistry 38 (1999) 12218.
[133] N. Lehnert, E.I. Solomon, J. Biol. Inorg. Chem. 8 (2003) 294.
[134] B. Su, E.H. Oliw, J. Biol. Chem. 273 (1998) 13072.
[135] M. Hamberg, C. Su, E. Oliw, J. Biol. Chem. 273 (1998) 13080.
[136] C.R. Goldsmith, R.T. Jonas, T.D.P. Stack, J. Am. Chem. Soc. 124 (2002) 83.
[137] C.R. Goldsmith, A.P. Cole, T.D.P. Stack, J. Am. Chem. Soc. 127 (2005) 9904.
[138] J.M. Mayer, Acc. Chem. Res. 37 (1998) 441.
[139] F.G. Bordwell, J.P. Cheng, J.A. Harrelson, J. Am. Chem. Soc. 110 (1988) 1229.
[140] Y. Feng, T.B. Gunnoe, T.V. Grimes, T.R. Cundari, Organometallics 25 (2006) 5456.
[141] S. Mukhopadhyay, S.K. Mandal, S. Bhaduri, W.H. Armstrong, Chem. Rev. 104 (2004) 3981.
[142] T.J. Hubin, J.M. McCormick, S.R. Collinson, M. Buchalova, C.M. Perkins, N.W. Alcock, P.K. Kahol, A. Raghunathan, D.H. Busch, J. Am. Chem. Soc. 122 (2000) 2512.
[143] T.J. Hubin, J.M. McCormick, S.R. Collinson, N.W. Alcock, H.J. Clase, D.H. Busch, Inorg. Chim. Acta 346 (2003) 76.
[144] S.R. Collinson, N.W. Alcock, T.J. Hubin, D.H. Busch, J. Coord. Chem. 52 (2001) 317.
[145] S.R. Collinson, N.W. Alcock, A. Raghunathan, P.K. Kahol, D.H. Busch, Inorg. Chem. 39 (2000) 757.
[146] T.J. Hubin, J.M. McCormick, N.W. Alcock, D.H. Busch, Inorg. Chem. 40 (2001) 435.
[147] H.T. He, G. Yin, G. Hiler, D. Kitko, J.D. Carter, W.M. Scheper, V. Day, D.H. Busch, J. Coord. Chem. 61 (2008) 45.
[148] G. Yin, J.M. McCormick, M. Buchalova, A.M. Danby, K. Rodgers, K. Smith, C. Perkins, D. Kitko, J. Carter, W.M. Scheper, D.H. Busch, Inorg. Chem. 45 (2006) 8052.
[149] G. Yin, A.M. Danby, D. Kitko, J.D. Carter, W.M. Scheper, D.H. Busch, J. Am. Chem. Soc. 129 (2007) 1512.
[150] G. Yin, A.M. Danby, D. Kitko, J.D. Carter, W.M. Scheper, D.H. Busch, J. Am. Chem. Soc. 130 (2008) 16245.
[151] A. Xu, H. Xiong, G. Yin, Chem. Eur. J. 15 (2009) 11478.
[152] T. Kurahashi, A. Kikuchi, T. Tosha, Y. Shiro, T. Kitagawa, H. Fujii, Inorg. Chem. 47 (2008) 1674.
[153] R. Gupta, A.S. Borovik, J. Am. Chem. Soc. 125 (2003) 13234.
[154] A.S. Borovik, Acc. Chem. Res. 38 (2005) 54.
[155] T.H. Parsell, M. Yang, A.S. Borovik, J. Am. Chem. Soc. 131 (2009) 2762.